Human ADA2 deficiency is characterized by the absence of an intracellular hypoglycosylated form of adenosine deaminase 2

Lisa Ehlers[1,2,3,4,5] (ORCID: 0000-0001-8737-001X), Anneleen Hombrouck[1] (ORCID: 0009-0003-5236-6063), Marjon Wouters[1] (ORCID: 0000-0002-4675-1665), Bethany Pillay[1] (ORCID: 0000-0001-7964-544X), Selket Delafontaine[1] (ORCID: 0000-0002-8985-8155), Giorgia Bucciol[1] (ORCID: 0000-0001-5004-0738), Marco Baggio[1,6] (ORCID: 0000-0001-6708-9925), Mariia Dzhus[1] (ORCID: 0000-0002-2077-4295), Frédéric Ebstein[7] (ORCID: 0000-0002-3729-7878), Maarten Jacquemyn[8] (ORCID: 0000-0003-2626-4189), Lien De Somer[9,10] (ORCID: 0000-0002-8488-5090), Rik Schrijvers[11] (ORCID: 0000-0002-4261-6220), Steven Vanderschueren[12] (ORCID: 0000-0002-4003-5465), David Cassiman[13] (ORCID: 0000-0002-6154-0970), Marieluise Kirchner[14] (ORCID: 0000-0002-7049-534X), Philipp Mertins[14] (ORCID: 0000-0002-2245-528X), Mir-Farzin Mashreghi[4,5] (ORCID: 0000-0002-8015-6907), Tilmann Kallinich[2,3,4,5] (ORCID: 0000-0003-2404-9397), Dirk Daelemans[8] (ORCID: 0000-0001-7092-1153), Patrizia Agostinis[15] (ORCID: 0000-0003-1314-2115), Leen Moens[1] (ORCID: 0000-0002-5347-6526), Isabelle Meyts[1] (ORCID: 0000-0003-1214-0302)

Affiliations:

1 Department of Microbiology, Immunology and Transplantation, Laboratory for Inborn Errors of Immunity, KU Leuven, Leuven, Belgium

2 Department of Pediatric Respiratory Medicine, Immunology and Critical Care Medicine, Charité – Universitätsmedizin Berlin, corporate member of Freie Universität Berlin and Humboldt-Universität zu Berlin, Berlin, Germany

3 Berlin Institute of Health at Charité – Universitätsmedizin Berlin, Berlin, Germany

4 German Center for Child and Adolescent Health (DZKJ), partner site Berlin, Berlin, Germany

5 Deutsches Rheuma-Forschungszentrum, an Institute of the Leibniz Association, Berlin, Germany

6 Laboratory of Computational and Developmental Biology, Berlin Institute for Medical Systems Biology (BIMSB), Max-Delbrück-Centrum for Molecular Medicine in the Helmholtz Association (MDC), Berlin, Germany

7 Nantes University, CHU Nantes, CNRS, INSERM, Nantes, France

8 KU Leuven Department of Microbiology, Immunology and Transplantation, Laboratory of Virology and Chemotherapy, Rega Institute for Medical Research, Leuven, Belgium

9 Department of Pediatric Rheumatology, University Hospitals Leuven, Leuven, Belgium

10 Laboratory of Immunobiology, Department of Microbiology and Immunology, KU Leuven, Leuven, Belgium

11 Department of Microbiology, Immunology and Transplantation, Allergy and Clinical immunology Research group, KU Leuven, Leuven, Belgium

12 Department of General Internal Medicine, Research Department Microbiology, Immunology, and Transplantation, Laboratory of Clinical Infectious and Inflammatory Disorders, University Hospitals Leuven, Leuven, Belgium

13 Department of Gastroenterology-Hepatology and Metabolic Center, University Hospital Leuven, Leuven, Belgium

14 Core Unit Proteomics, Berlin Institute of Health at Charité - Universitätsmedizin Berlin and Max-Delbrück-Center for Molecular Medicine, Berlin, Germany

15 Cell Death Research & Therapy (CDRT) Lab, Department of Cellular & Molecular Medicine, Center for Cancer Biology, VIB-KU Leuven, Leuven, Belgium

Corresponding author:

Isabelle Meyts, Laboratory for Inborn Errors of Immunity and Department of Pediatrics UZ Leuven, Herestraat 49, 3000 Leuven, Belgium; Tel +32 16 343841; Fax +32 16 343842; isabelle.meyts@uzleuven.be

Abstract

Human deficiency of adenosine deaminase 2 (DADA2) is a rare autoinflammatory disease with a complex clinical phenotype of recurrent fever, vasculitis and stroke as well as immunodeficiency and bone marrow failure. It is caused by pathogenic variants in *ADA2* that lead to impaired ADA2 protein secretion and reduced deaminase activity. However, the mechanisms driving the disease on a cellular level remain elusive. Here, we analyze protein expression of mutant ADA2 in human monocyte-derived macrophages from 10 DADA2 patients. We identify a low-molecular-weight (LMW) form of ADA2 expressed exclusively intracellularly in healthy control macrophages. This LMW-ADA2 is subject to glycan trimming by α-mannosidases after transfer to the Golgi and is distinct from secreted high-molecular-weight (HMW) ADA2. DADA2 patients' monocyte-derived macrophages lack LMW-ADA2 and mutant ADA2 does not undergo glycan processing in the Golgi. We confirm the absence of LMW-ADA2 upon overexpression of 11 pathogenic *ADA2* variants in HEK293T cells and monocytic U-937 cells. By subcellular fractionation, we show that LMW-ADA2 localizes to the cytosolic and lysosomal compartments. In conclusion, we describe a previously unreported intracellular hypoglycosylated form of ADA2 and establish the absence of this LMW-ADA2 as a cellular characteristic of DADA2.

Introduction

Human deficiency of adenosine deaminase 2 (DADA2) is an inborn error of immunity caused by biallelic deleterious mutations in the *ADA2* gene *(1, 2)*. The disease manifests with a diverse phenotype displaying features of both autoinflammation and immunodeficiency *(3)*. More than 600 missense or predicted loss-of-function variants in *ADA2* are listed in the Genome Aggregation Database (gnomAD v4.1.0) *(4)*. In the Infevers registry, 116 *ADA2* variants are classified as (likely) pathogenic *(5)*. Complete loss-of-function variants are more likely to cause bone marrow failure. Missense variants which account for 80% of pathogenic variants are found in patients with a primarily vasculitis phenotype as well as in those presenting with cytopenias and hypogammaglobulinemia *(6, 7)*.

How mutations in *ADA2* give rise to this diverse phenotype, even in patients with identical genotypes, is not understood. Inflammatory symptoms of the disease typically respond well to TNF inhibitors (TNFi) *(8)*. Insufficient resolution of bone marrow failure in response to this treatment however often necessitates hematopoietic stem cell transplantation and disease lethality still is 8% *(9)*. To develop improved treatment options, we require a better understanding of the pathomechanisms underlying the immunological and clinical phenotype of DADA2.

ADA2 is a 59-kD glycoprotein with a signal peptide that mediates secretion of the protein via the endoplasmic reticulum (ER), and exhibits extracellular adenosine deaminase activity as a homodimer *(10)*. The protein has four N-glycosylation sites and insufficient glycosylation leads to ER retention and intracellular aggregate formation of ADA2 transfected into HEK293T cells *(11, 12)*. Impaired protein secretion and absent serum ADA2 enzyme activity have been established as characteristics shared by the majority of pathogenic ADA2 variants *(13)*. Mechanistic approaches to the pathophysiology of ADA2-deficient cells have therefore been based on impaired extracellular adenosine deamination driving inflammation *(14, 15)*. This assumption fails to acknowledge the weak affinity of ADA2 for adenosine and the presence of functional ADA1 in

DADA2 patients *(16)*. Research into alternative functions of the ADA2 protein and DADA2-causing variants is therefore warranted. Biochemical characterization of pathogenic *ADA2* variants has until now mostly been performed in a HEK293T overexpression system with supraphysiological intracellular levels of ADA2 while expression of the mutant protein has been shown to be minimal in DADA2 CD14+ monocytes *(13, 17)*. Disease-associated ADA2 variants have to date hardly been studied in their physiological milieu.

In this study, we analyze trafficking and glycosylation of endogenous ADA2 expressed in primary human macrophages from healthy donors and DADA2 patients. We provide evidence of an intracellular glycoform of ADA2 that results from glycan trimming by Golgi α-mannosidases and show that DADA2 macrophages are characterized by the absence of this low-molecular-weight-form of ADA2.

Results

In vitro macrophage differentiation partially restores ADA2 protein expression in DADA2 monocytes

Of the circulating leukocytes, monocytes express ADA2 most abundantly. We analyzed ADA2 protein expression and *ADA2* mRNA levels in peripheral blood monocytes of 10 DADA2 patients and three heterozygous carriers (**Table 1** and **Figure S1A+B**). CD14+ monocytes from DADA2 patients showed very low or absent ADA2 protein expression despite normal *ADA2* mRNA levels in patients with missense mutations which account for 80% of pathogenic variants found in DADA2 patients (**Figure 1A** and **Figure S2A**). Upon macrophage differentiation, we observed an increase in mutant ADA2 protein expression in the patient cells while ADA2 protein expression was reduced in healthy control (HC) human monocyte-derived macrophages (HMDM) (**Figure 1B**). Successful differentiation of DADA2 HMDM was achieved both with granulocyte–macrophage colony-stimulating factor (GM-CSF) and macrophage colony-stimulating factor (M-

CSF) (**Figure S2B**), which confirms the reported restoration of macrophage differentiation of monocytes from DADA2 patients under treatment with TNFi *(8)*. Interestingly, western blotting of pathogenic ADA2 protein variants expressed in DADA2 HMDM revealed the presence of only a high-molecular-weight (HMW) band of around 60 kD compared to HC HMDM displaying two bands at 60 and 57 kD, with the low-molecular-weight (LMW) band being more pronounced (**Figure 1B** and **Figure S2C**). A novel ADA2 variant serendipitously created in the process of generating an ADA2$^{-/-}$ Jurkat cell line showed the same phenotype (**Figure S2D**). The molecular weight of secreted wild-type (WT) ADA2 in the supernatant of HC HMDM corresponded to the intracellular HMW form – the only form expressed in DADA2 HMDM (**Figure 1B**). We confirmed the secretion of HMW-ADA2 in the monocytic cell lines U-937 and THP-1 (**Figure S2E**). HMDM from DADA2 patient P8 showed residual secretion of HMW-ADA2 with a molecular weight equivalent to secreted WT ADA2 (**Figure S2F**). This HMW-form of ADA2 also corresponded to the ADA2 form detected in human serum (**Figure 1C**). Importantly, overexpression of tagged WT ADA2 and several confirmed pathogenic variants in HEK293T cells uniformly led to predominant intracellular expression of HMW-ADA2 (63 kD) which was equal in size to the secreted protein (**Figure 1D**). In line with our findings in DADA2 HMDM, intracellular LMW-ADA2 was absent after overexpression of mutant ADA2 in HEK293T cells (**Figure 1D**). Interestingly, this band was still present – albeit at lower intensity – in the variants p.N127Q and p.W326R, two variants not found in DADA2 patients but created for the study of ADA2 glycosylation and dimerization, respectively *(10, 11)*. Collectively, we show that HC HMDM intracellularly express a form of ADA2 that is lower in molecular weight than the secreted protein. This LMW-form is absent in DADA2 HMDM which only express the HMW-form intracellularly.

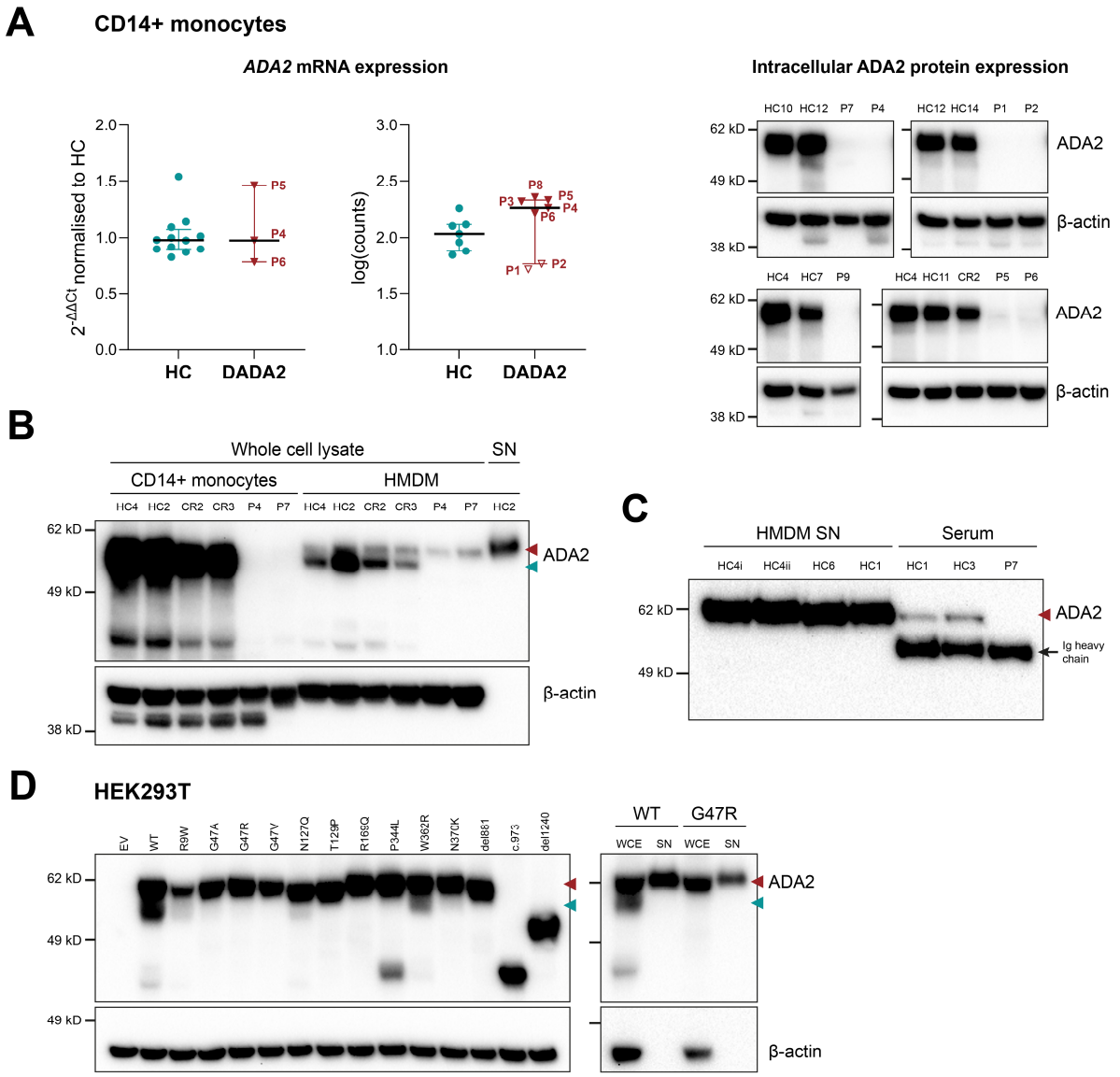

Figure 1: Expression of pathogenic ADA2 protein variants. (A) mRNA and intracellular protein expression of ADA2 in CD14+ monocytes from healthy controls (HC) and DADA2 patients (P) by qPCR or bulk RNA-sequencing and western blot of whole cell lysates, respectively. The left plot shows mRNA expression determined by qPCR. *ADA2* mRNA expression was normalized to *GAPDH* and is depicted relative to the mean of HC samples. The right plot shows counts determined by RNA-sequencing. Dot plots show median and interquartile range. (B) ADA2 protein expression in whole cell lysates and supernatant (SN) of CD14+ monocytes and GM-CSF differentiated human monocyte-derived macrophages (HMDM) from healthy controls (HC), carriers (CR) and DADA2 patients (P) was determined by western blot. (C) ADA2 protein expression in supernatants (SN) from healthy control human monocyte-derived macrophages (HMDM) and serum samples from healthy controls (HC) and DADA2 patients (P) by western blot using VeriBlot for detection. (D) ADA2 protein expression in whole cell lysates of HEK293T cells after transfection with wild-type (WT) ADA2 and different pathogenic variants (*left*) and comparing whole cell lysates (WCE) and supernatant (SN) by western blot (*right*). Triangles indicate HMW-ADA2 (red) and LMW-ADA2 (green). Legend: Ig, immunoglobulin.

Human monocyte-derived macrophages intracellularly express a hypoglycosylated low-molecular-weight form of ADA2 that is absent in DADA2 macrophages

Differences in the molecular weight of a protein can be caused by posttranslational protein modifications and N-glycosylation of ADA2 has previously been confirmed *(10, 12, 17)*. Therefore, we initially hypothesized that the LMW-form of ADA2 unique to cells expressing WT ADA2 corresponded to glycan-free ADA2. To test this, we performed glycan removal on lysates and supernatants containing ADA2 protein. Complete removal of N-glycans by Peptide-N-Glycosidase F (PNGase F) yielded a difference in molecular weight of 7 kD between HMW-ADA2 and glycan-free ADA2 both overexpressed in HEK293T cells and endogenously expressed in the monocytic cell lines U-937 and THP-1 as well as HMDM (**Figure 2A+B**), revealing that LMW-ADA2 was in fact slightly larger than glycan-free ADA2. Importantly, the anti-ADA2 antibody clone EPR25430-131 (#ab288296; abcam) was superior in detecting LMW-ADA2 but poorly detected glycan-free ADA2 (**Figure S3A**). Glycan removal by PNGase F eliminated the differences in molecular weight between the LMW-form and the HMW-form in HMDM, yielding a single band of glycan-free ADA2 at 53 kD (**Figure 2B+C**). Hence, the difference in molecular weight between intracellular WT ADA2 (LMW) and secreted WT ADA2 or intracellular pathogenic ADA2 (both HMW) was due to differential protein glycosylation. Of note, glycan removal yielded a smaller band of 53 kD in addition to the glycan-removed 56 kD protein for tagged WT ADA2 overexpressed in HEK293T cells that was absent for all tested pathogenic variants and did not appear after inhibition of N-glycosylation by tunicamycin (**Figure 2A**). As this band was absent after glycan removal of endogenous WT ADA2, its physiological relevance is unclear.

Overall, we showed that the difference in size between HMW- and LMW-ADA2 is due to differential protein glycosylation.

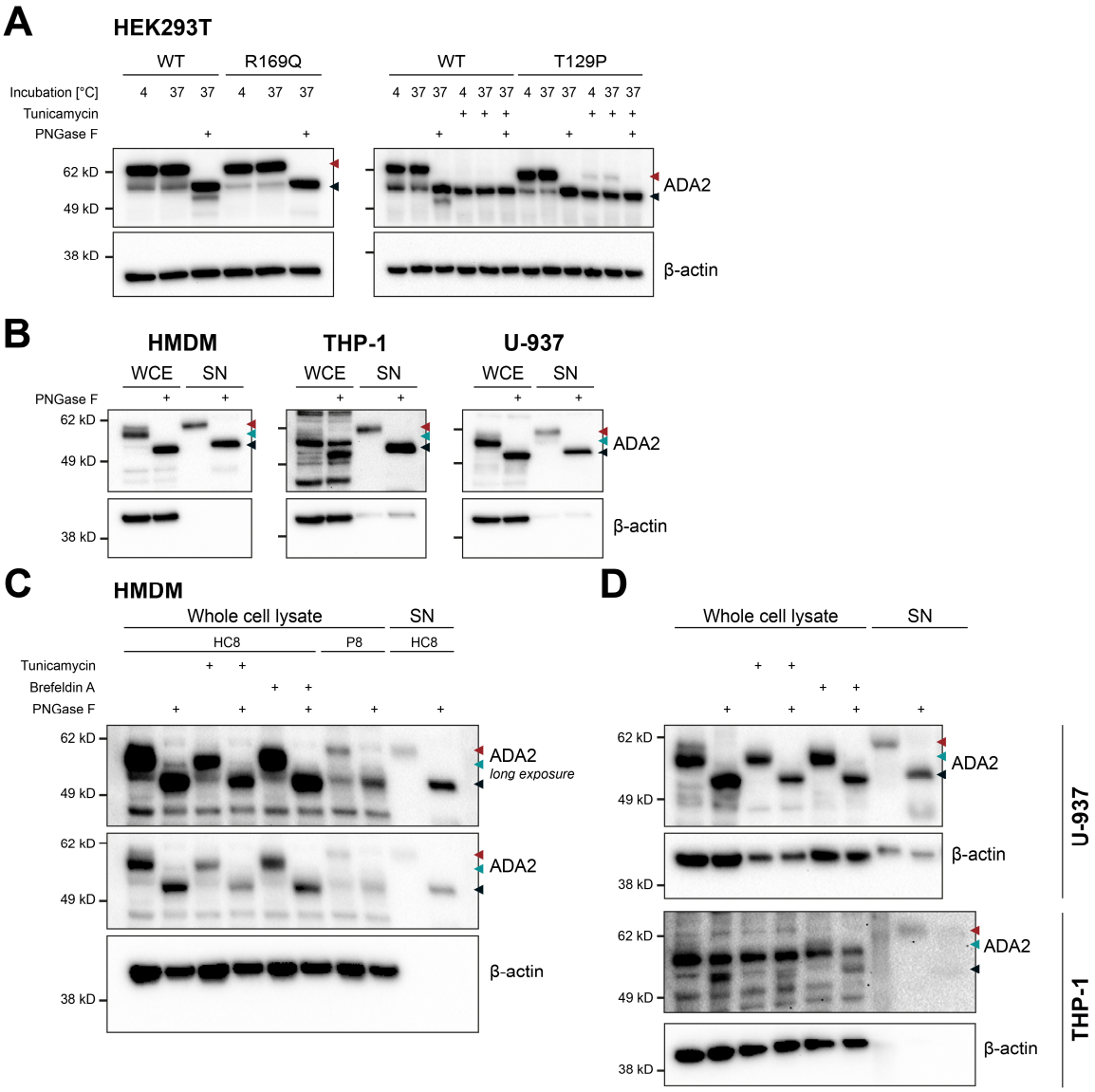

Figure 2: N-glycosylation pattern of ADA2. (A) Western blot of wild-type (WT) ADA2 and the pathogenic variants p.R169Q and p.T129P transfected into HEK293T cells after incubation with or without 2.5 µg/mL tunicamycin (TM) for 24h. (B) ADA2 protein expression by western blot in whole cell lysates (WCE) and supernatants (SN) of human monocyte-derived macrophages (HMDM), U-937 cells and THP-1 cells. (C) ADA2 protein expression in whole cell lysates and supernatants (SN) from GM-CSF-differentiated HMDM of healthy control HC8 and DADA2 patient P8 left untreated or treated with 5 µg/mL tunicamycin or 1 µg/mL brefeldin A for 24h. (D) ADA2 protein expression in whole cell lysates and supernatants (SN) from U-937 and THP-1 cells left untreated or treated with 2.5 µg/mL tunicamycin or 1 µg/mL brefeldin A for 24h. Glycan removal was performed by incubation with PNGase F for 1 hour at 37°C under denaturing conditions in all experiments. Triangles indicate HMW-ADA2 (red), LMW-ADA2 (green) and glycan-free ADA2 (dark blue).

N-glycosylated ADA2 undergoes glycan trimming in the ER as part of protein quality control

In order to better characterize the glycosylation of endogenous ADA2, we inhibited N-glycosylation in HMDM and the monocytic cell lines U-937 and THP-1 by 24-hour treatment with tunicamycin. We found that this treatment only acted on the fainter HMW-band while LMW-ADA2 remained unchanged in size (**Figure 2C+D**). In accordance with previous findings *(12)*, we showed that adenosine deaminase activity of ADA2 was preserved after glycan removal while treatment with tunicamycin reduced enzymatic activity. This was true for ADA2 overexpressed in HEK293T cells as well as endogenous ADA2 from HC HMDM (**Figure 3A+B**). These findings indicated that N-glycosylation was required for adequate folding of the ADA2 protein. The ER glucosidases I and II form part of the ER quality control by removing glycosyl residues from accurately folded proteins prior to transfer to the Golgi apparatus *(18)*. Treatment with castanospermine, an inhibitor of the ER glucosidases I and II, caused an additional increase in the size of HMW-ADA2 in both HC and DADA2 HMDM (**Figure 3C**), confirming trimming of N-glycosylated ADA2 in the ER. Since the same shift in molecular weight was observed in DADA2 HMDM, we concluded that processing of WT and mutant did not yet diverge at this early stage of the secretory pathway. As seen previously upon incubation with tunicamycin, the LMW-form of ADA2, which is absent in DADA2 HMDM, was unaffected by this treatment (**Figure 3C**). We confirmed this finding in the three ADA2-expressing cell lines U-937, THP-1 and Jurkat (**Figure 3D**). Following glycan processing in the ER, proteins exit the ER to the Golgi apparatus. ER to Golgi trafficking is inhibited by brefeldin A (BFA). We observed that treatment of WT ADA2-expressing cells with BFA yielded a single ADA2 band with a molecular weight between that of HMW- and LMW-ADA2 (**Figure 3D**), suggesting that both HMW- and LMW-ADA2 are the result of further glycan processing in the Golgi. In summary, we showed that N-glycosylation is required for folding and secretion of ADA2 and that both WT and mutant ADA2 are subject to processing by the ER glucosidases I and II.

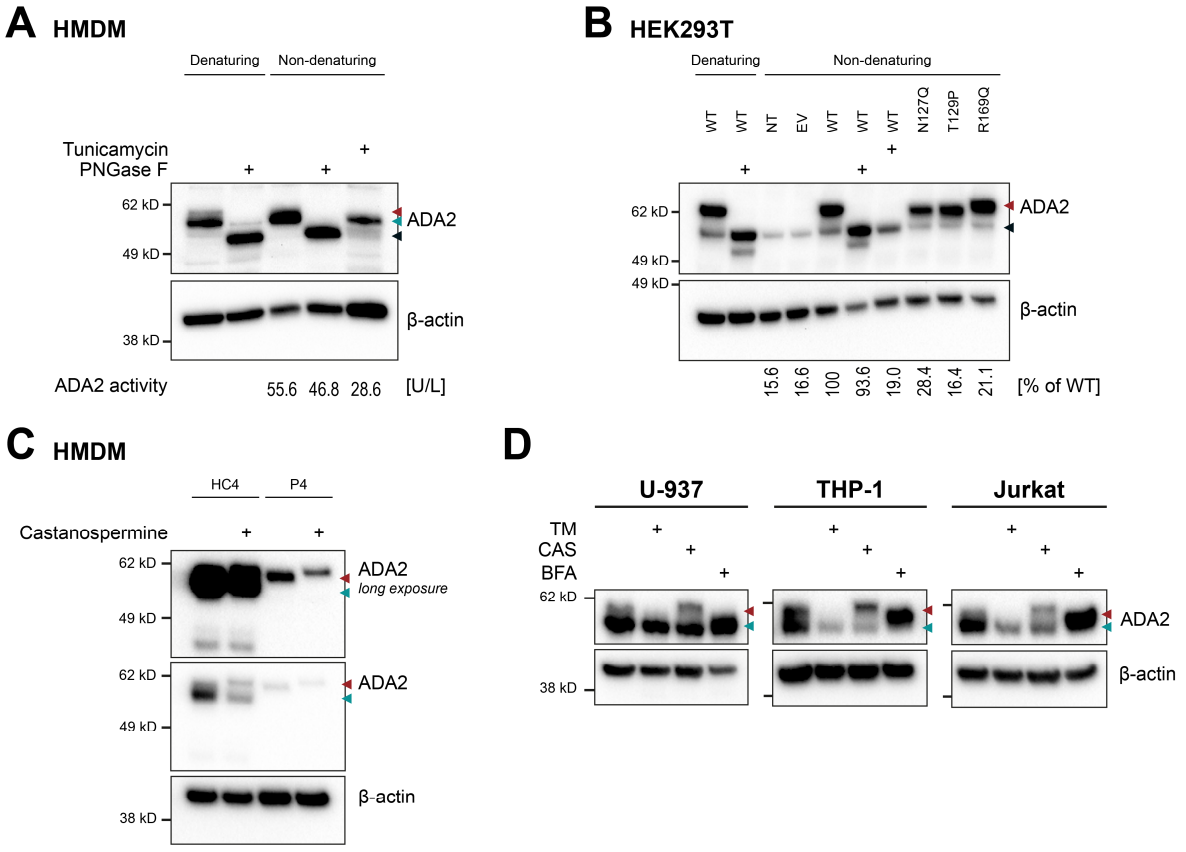

Figure 3: Glycan processing of ADA2 in the ER. GM-CSF-differentiated healthy control HMDM (A) or HEK293T cells transfected with wild-type (WT) *ADA2* or pathogenic *ADA2* variants (B) were treated with or without 5 µg/mL and 2.5 µg/mL tunicamycin for 24h, respectively. Glycan removal was performed by incubation with PNGase F at 37°C under denaturing (1h) and non-denaturing (4h) conditions. ADA2 enzyme activity was determined in whole cell lysates handled under non-denaturing conditions. (C) ADA2 protein expression by western blot in GM-CSF-differentiated HMDM from healthy control HC12 and DADA2 patient P4 after incubation with 100 µg/mL castanospermine for 24h. (D) ADA2 protein expression upon inhibition of N-glycosylation, ER glucosidase I and II, or ER to Golgi trafficking. U-937, THP-1 and Jurkat cells were incubated with 2.5 µg/mL tunicamycin (TM), 100 µg/mL castanospermine (CAS) or 1 µg/mL brefeldin A (BFA) for 24h. Triangles indicate HMW-ADA2 (red), LMW-ADA2 (green) and glycan-free ADA2 (dark blue). Legend: EV, empty vector; NT, non-transfected.

Inhibition of ER to Golgi trafficking partially reproduced the ADA2 proteotype of DADA2 cells

Since the glycan pattern of LMW-ADA2 was unaffected by treatment with tunicamycin – an inhibitor of the initial step of N-glycosylation – we concluded that glycosylation of this form must have occurred prior to the treatment incubation period, suggesting high stability of LMW-ADA2. Accordingly, LMW-ADA2 was responsive to prolonged incubation with tunicamycin at a lower

concentration (**Figure S3B**). The same was true for inhibition of ER glucosidases: the more stable LMW-ADA2 was unaffected by 24-hour incubation with castanospermine and the detected LMW-form had likely already matured before the beginning of the incubation period. The increased stability of LMW-ADA2 compared to HMW-ADA2 was also confirmed by cycloheximide chase assay (**Figure S4A**). Besides, this experiment revealed that HMW-ADA2 protein expressed by HEK293T cells transfected with pathogenic *ADA2* variants showed increased intracellular stability compared with the WT protein. This was also true after inhibition of N-glycosylation and after an increased incubation period of 48 hours (**Figure S4B+C**). Since ADA2 is a secreted protein, protein secretion must be taken into account when assessing the intracellular signal reduction in this assay over time. Impaired secretion has previously been established as a characteristic of pathogenic ADA2 variants *(2, 13)*. We confirmed the secretory defect in HMDM from our DADA2 cohort (**Figure 4A**). Overexpression in HEK293T cells recapitulated the endogenous behavior of the respective variants well (**Figure 4A**). While residual ADA2 enzyme activity largely correlated with preserved secretion, the catalytic domain variant p.N370K displayed absent deaminase activity despite comparatively high protein levels in the supernatant (**Figure 4A**). The partially preserved secretion of the variant p.G47R *(2)* was verified in HMDM from patient P8 who is homozygous for this variant (**Figure 4A**) and corresponded to higher serum ADA2 levels (**Figure 4A**) in the absence of serum deaminase activity (0.3 U/L).

Comparing the levels of increased ADA2 stability observed by cycloheximide chase assay with residual protein secretion, the variants p.T129P and p.R169Q that exhibited complete absence of secretion did indeed show the highest levels of intracellular ADA2 24 hours after inhibition of protein synthesis (**Figure S4A**). However, intracellular levels of the secreted mutant p.P344L were still higher compared to WT. By blocking the secretory pathway to impair secretion of WT ADA2, we confirmed that the secretory defect strongly contributed to the increased intracellular protein levels of mutant ADA2 (**Figure 4B and S4D**). As described above, this treatment also hindered the generation of LMW-ADA2. Consequently, inhibition of ER to Golgi trafficking by BFA

mimicked major characteristics of ADA2 processing in DADA2 cells: ER retention, impaired secretion and absence of LMW-ADA2. Besides incomplete glycan processing and ER retention, aggregate formation can be a consequence of protein misfolding *(19)*. Upon overexpression of mutant ADA2 in HEK293T cells, we observed intracellular ADA2 dimer formation by western blot of whole cell lysates (**Figures S5+6**).

Overall, we demonstrated that LMW-ADA2 exhibits increased intracellular stability, and that impairment of protein trafficking mirrored the cellular DADA2 phenotype to a certain extent.

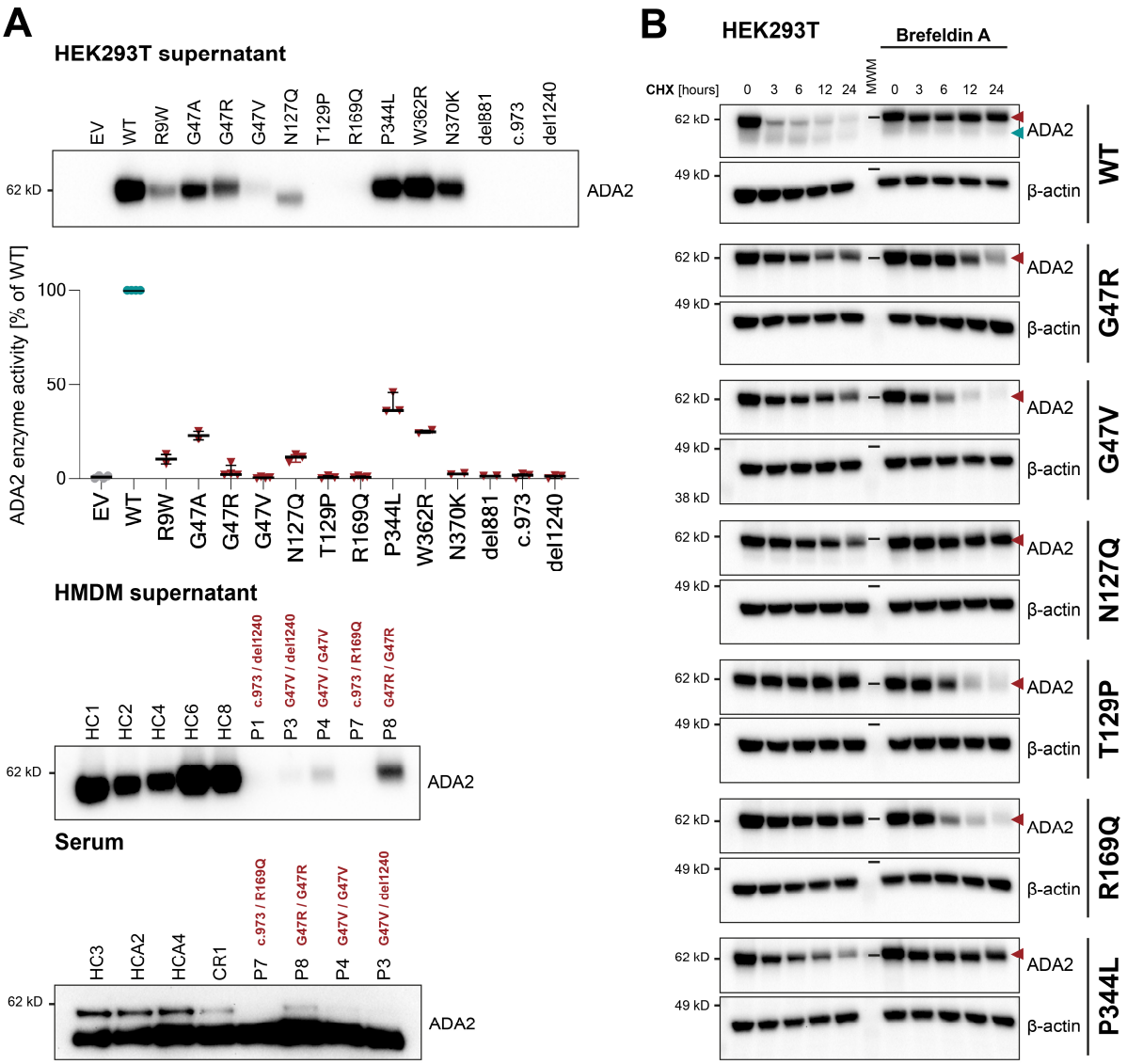

Figure 4: Trafficking of ADA2. (A) ADA2 protein levels were determined in supernatants of M-CSF-differentiated human monocyte-derived macrophages (HMDM) from healthy controls (HC) or DADA2 patients (P) or HEK293T cells transfected with wild-type (WT) ADA2 or different pathogenic ADA2 variants. The patients' genotypes are indicated above. ADA2 enzyme activity was determined in the supernatant. Data are shown from n=2-4

independent experiments. Dot plots show median and interquartile range. Western blot of serum samples from healthy controls (HC), heterozygous DADA2 carriers (CR) and DADA2 patients (P) detected by anti-ADA2 antibody clone EPR25430-131 (#ab288296; abcam) and VeriBlot. (B) HEK293T cells were transfected with wild-type (WT) ADA2 or different pathogenic variants and treated with 500 µg/mL cycloheximide (CHX) ± 1 µg/mL brefeldin A (BFA) over 24h. Whole cell lysates were generated at the indicated time points and immunoblotted for ADA2 expression. Triangles indicate HMW-ADA2 (red), LMW-ADA2 (green) and glycan-free ADA2 (dark blue). Legend: EV, empty vector; MWM, molecular weight marker.

The pathogenic ADA2 variant p.R169Q shows increased binding to proteins of the protein folding machinery

Protein misfolding is known to cause ER stress and induce the unfolded protein response (UPR). We performed immunoprecipitation followed by mass spectrometry (IP-MS) to analyze the interactome of WT ADA2 and the pathogenic variant p.R169Q transfected into HEK293T cells. p.R169Q displayed increased interaction with proteins involved in the ER quality control machinery for glycoproteins (**Figure 5A** and **Table S1**). Upon inhibition of N-glycosylation by tunicamycin, we observed a similar increase also for the WT protein (**Figure 5A** and **Table S1**), highlighting the importance of adequate N-glycosylation for successful folding and secretion of ADA2. Additionally, we observed an increase in lysosomal proteins in the ADA2 interactome after treatment with tunicamycin, suggesting autophagic degradation of non-glycosylated ADA2. Among the induced interactors were several proteins of the chaperone-mediated autophagy pathway, e.g. LAMP2 and HSPA13, and we verified the presence of a KFERQ-related motif (QKFVE, amino acids 274-278) in the sequence of ADA2 *(20)*. IP-MS of HC and DADA2 HMDM did not yield any specific binders, which was possibly due to low protein abundance in the pull down of endogenous ADA2 (**Figure S7A**). Notably, IP preferentially pulled down the HMW-form of ADA2 (**Figure S7B+C**). The experiment consequently did not allow us to draw conclusions about the interactome and potential distinctive function of LMW-ADA2.

Given the increased binding of mutant ADA2 to the ER folding machinery, we verified whether pathogenic ADA2 variants induced an increased ER stress response. In line with previous reports *(13)*, we observed that some pathogenic *ADA2* variants caused signs of activation of an ER stress

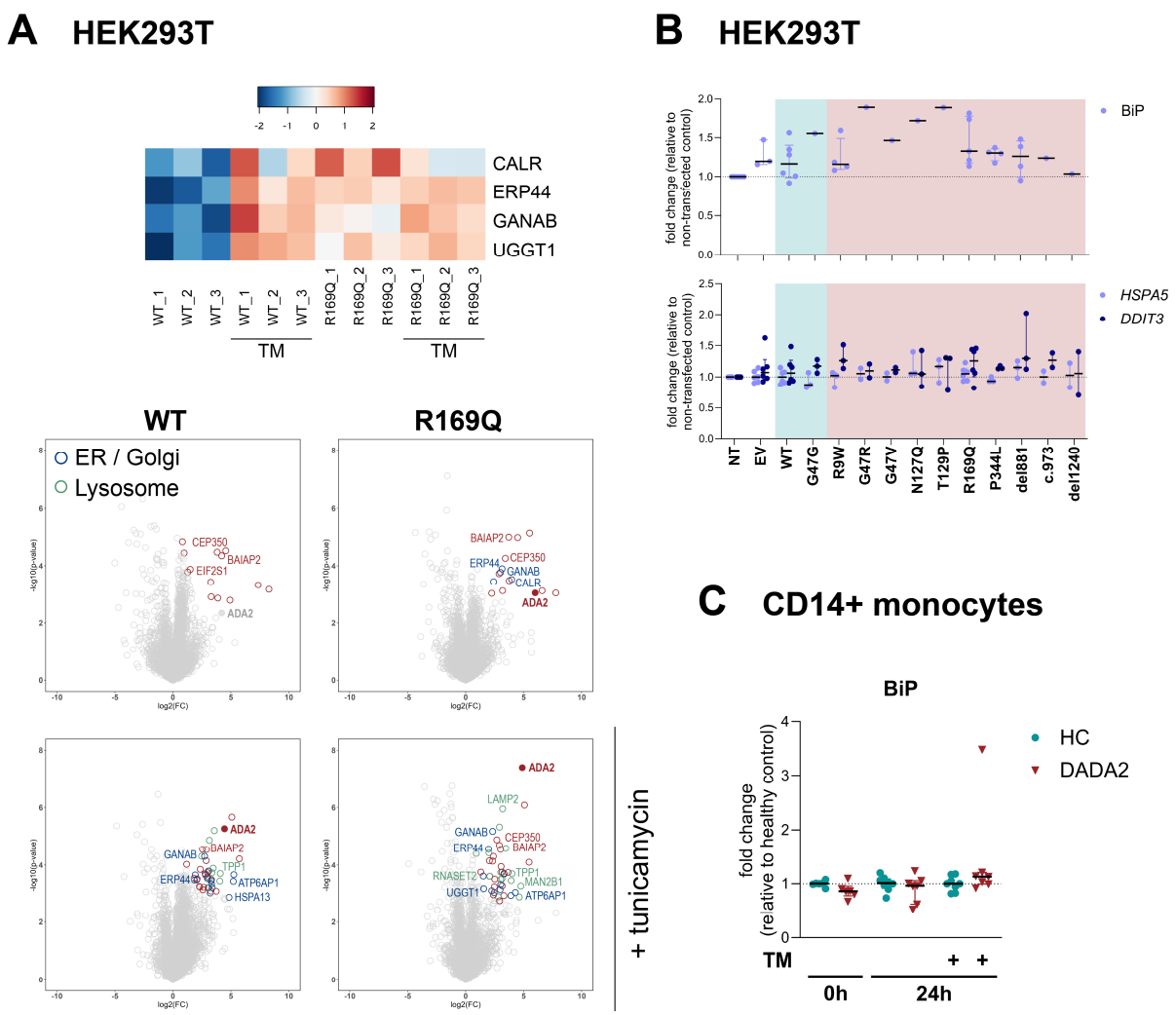

Figure 5: ER stress in DADA2. (A) Interactome analysis of wild-type (WT) ADA2 and the pathogenic variant p.R169Q overexpressed in HEK293T cells treated with or without 2.5 µg/mL tunicamycin (TM) for 24h was performed by immunoprecipitation followed by mass spectrometry. Heatmap shows z-score of protein abundance. Binders significantly pulled down compared to isotype control with a false discovery rate of 5% are highlighted by colored circles. Localization of the interacting proteins to the ER/Golgi (blue) or lysosome (green) is indicated by color. (B) ER stress response in HEK293T cells transfected with wild-type (WT) *ADA2* and different pathogenic variants. Protein expression of BiP (*top*) and mRNA expression of *HSPA5* and *DDIT3* (*bottom*) were determined 48h after transfection. A representative western blot is shown in **Figure S8C**. mRNA expression was normalized to *GAPDH* and is depicted as $2^{-\Delta\Delta Ct}$ relative to non-transfected control samples. Results from 6 independent experiments are shown. Dot plots show median and interquartile range. (C) ER stress response was evaluated by protein expression of BiP in whole cell lysates of CD14+ monocytes at baseline or after 24h incubation with or without 1 µg/mL tunicamycin (TM). BiP expression was normalized to β-actin. Dot plots show median and interquartile range. The corresponding western blots are shown in **Figure S9**. Legend: EV, empty vector; FC, fold change; NT, non-transfected.

response, measured by increased levels of CHOP (*DDIT3*) and BiP (*HSPA5*) (**Figure S8A**). These differences were however no longer present after down-titrating the amount of transfected DNA to achieve near-physiological protein levels (**Figure 5B** and **S8B+C**) and neither was there a difference in BiP expression in CD14+ monocytes from DADA2 patients compared to healthy controls (**Figure 5C** and **S9**). In summary, our experiments revealed the interaction of the ADA2 variant p.R169Q overexpressed in HEK293T cells with mediators of the folding machinery and ER quality control despite lack of increased ER stress in the presence of pathogenic ADA2 variants. The interactome analyses were inconclusive regarding potential alternative functions of LMW-ADA2.

LMW-ADA2 is generated from HMW-ADA2 after transfer to the Golgi and localizes to the lysosome

We showed that the secretory defect of mutant ADA2 was phenocopied by WT ADA2 upon inhibition of the secretory pathway by BFA (**Figure 4B**). However, this treatment also caused increased degradation of the mutants p.G47V, p.T129P and p.R169Q (**Figure 4B**). To determine whether this effect was specific to brefeldin A, we also inhibited protein trafficking with monensin. BFA blocks protein transport from the ER to the Golgi apparatus while monensin inhibits trans Golgi transport *(21, 22)*. Treatment with monensin also caused intracellular retention of WT ADA2 but protein levels of mutant ADA2 were unaffected (**Figure 6A**). The differential behavior in response to the secretory pathway inhibitors BFA and monensin was confirmed in DADA2 HMDM (**Figure 6B**). Moreover, unlike BFA, incubation with monensin did not impair the generation of LMW-ADA2 in cells overexpressing WT ADA2. The absence of LMW-ADA2 upon inhibition of ER to Golgi trafficking and the increase in LMW-ADA2 upon inhibition of trans Golgi transport indicated that the hypoglycosylated LMW-form is generated from HMW-ADA2 after transport to the Golgi apparatus. In order to better understand the subcellular localization of

LMW-ADA2, we performed subcellular fractionation experiments. We showed that HMW-ADA2 localized exclusively to the membranous fraction that also contains ER and Golgi membrane proteins (**Figure 6C**). LMW-ADA2 was also present in the membrane fraction. Moreover, this form was strongly detected in the cytosolic and lysosomal extracts. Considering that LMW-ADA2 only emerges at a later stage of the secretory pathway and localizes to different cellular compartments than the HMW-form, it is unlikely that LMW-ADA2 represents an intermediate – not yet fully glycosylated – form of yet unsecreted ADA2. Instead, we hypothesize that it is generated by partial intracellular glycan trimming of the fully glycosylated form (**Figure 6D**). Overall, we showed that ER to Golgi transport is required for the synthesis of LMW-ADA2 and that this ADA2-form is found in the lysosomes.

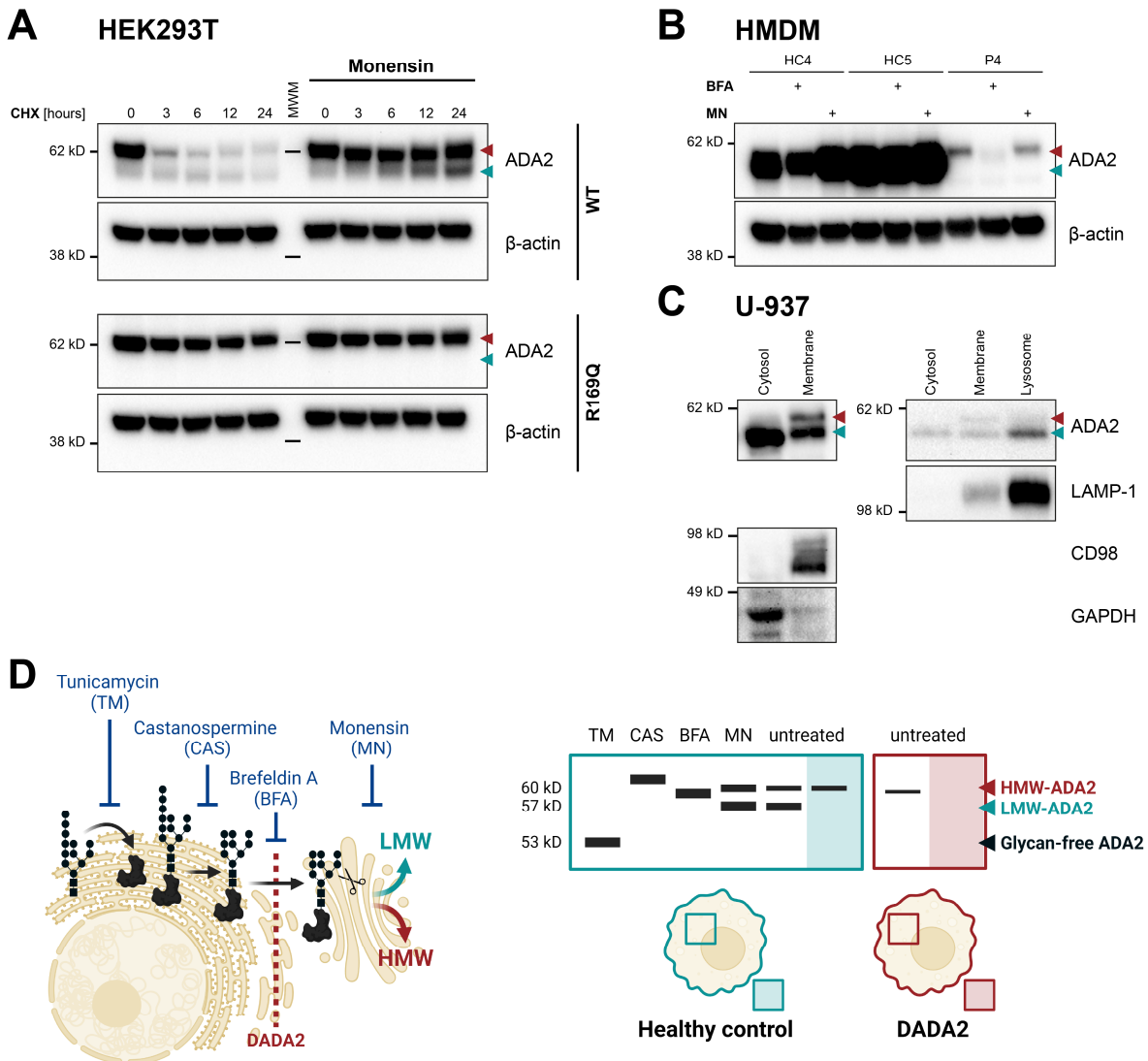

▲ **Figure 6: Trafficking and localization of HMW- and LMW-ADA2.** (A) HEK293T cells were transfected with wild-type (WT) ADA2 or the pathogenic variant p.R169Q and treated with 500 µg/mL cycloheximide (CHX) ± 2 µg/mL monensin for 24h. Whole cell lysates were generated at the indicated time points and immunoblotted for ADA2 expression. (B) ADA2 protein expression in GM-CSF-differentiated human monocyte-derived macrophages from healthy controls (HC) or DADA2 patient P4 left untreated or treated with 1 µg/mL brefeldin A (BFA) or 2 µg/mL monensin (MN). (C) ADA2 protein expression in cytosolic, membranous and lysosomal fractions of U-937 cells. (D) Schematic overview of the analysis of ADA2 protein trafficking and processing. Triangles indicate HMW-ADA2 (red) and LMW-ADA2 (green). Legend: HMW, high molecular weight; LMW, low molecular weight; MWM, molecular weight marker.

Wild-type HMW-ADA2 is subject to additional glycan maturation prior to secretion

Because of the differences observed in the processing of mutant ADA2 expressed in HEK293T cells or primary HMDM as well as the limitations of the HEK293T model system, we created a CRISPR/Cas9-mediated knock out of *ADA2* in U-937 cells, a monocytic cell line with endogenous ADA2 levels similar to those measured in HMDM. These ADA2$^{-/-}$ U-937 cells were then transduced with different pathogenic *ADA2* variants. We showed that expression levels of the mutant protein in these cells came very near to DADA2 HMDM (**Figure 7A**). Moreover, this model system excellently mirrored the expression pattern of WT and mutant ADA2 with respect to LMW- and HMW-ADA2. ADA2$^{-/-}$ U-937 cells transduced with the pathogenic *ADA2* variants p.G47R, p.G47V and p.R169Q expressed only HMW-ADA2 while LMW-ADA2 was the predominant form found in U-937 cells endogenously expressing WT ADA2 or transduced with WT after *ADA2* knockout (**Figure 7A**). The stability of LMW-ADA2 upon 24-hour incubation with tunicamycin was also reproduced (**Figure 7A**). In this system, we endeavored to confirm and extend our findings with respect to the ADA2 glycoforms: First, we showed that complete N-glycan removal by PNGase F cancelled out the differences in molecular weight between HMW- and LMW-ADA2, confirming that they are due to N-glycosylation. Endo H is another endoglycosidase that cleaves high mannose glycans and – unlike PNGase F – does not remove complex glycans. We found that WT and mutant ADA2 were both sensitive to glycan removal by Endo H (**Figure 7B**), hinting at the presence of high mannose oligosaccharides in both LMW- and HMW-ADA2 glycans. In contrast with PNGase F treatment, glycan removal by Endo H revealed

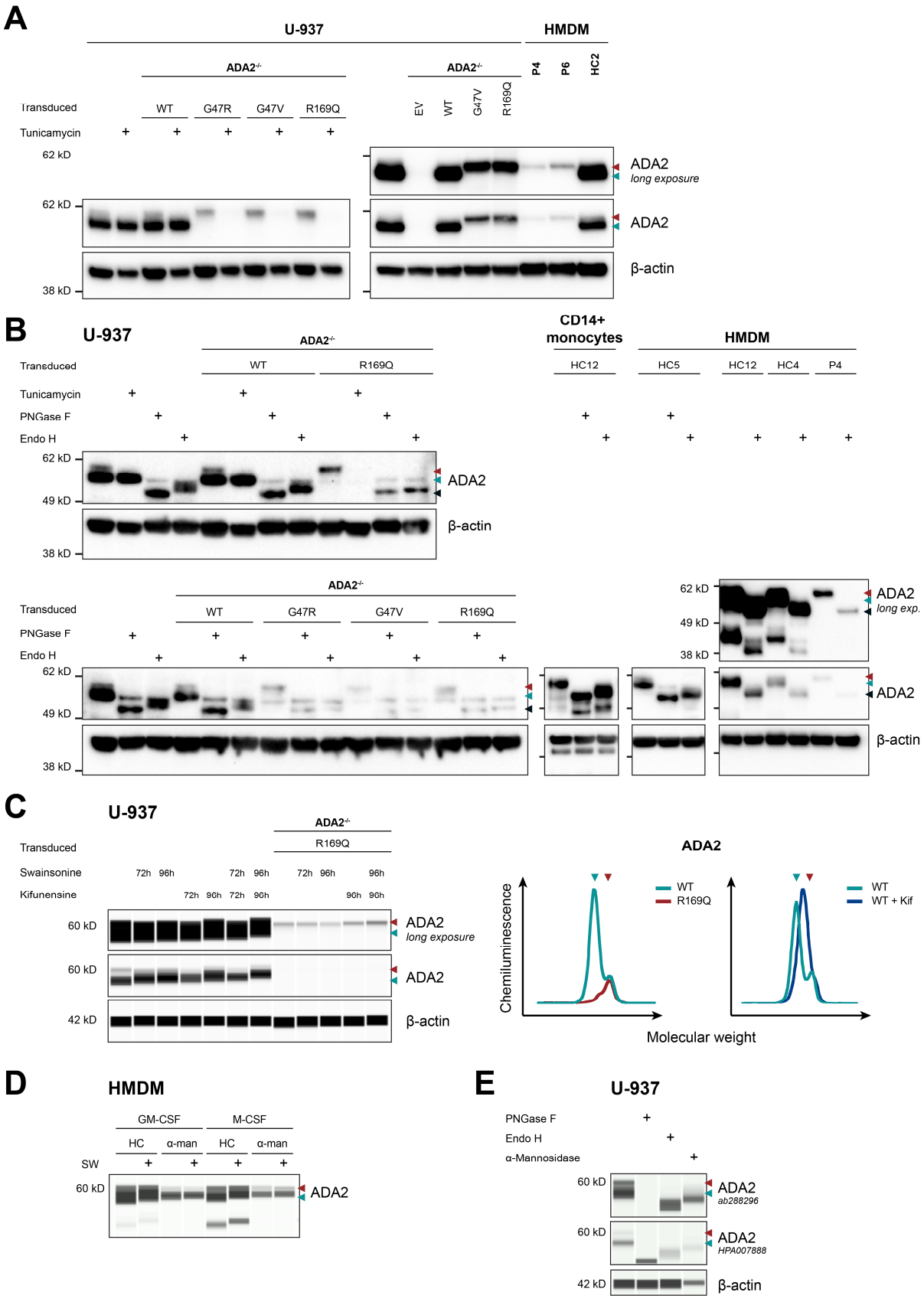

Figure 7: Glycan-processing of LMW-ADA2. (A) ADA2$^{WT/WT}$ and ADA2$^{-/-}$ U-937 cells transduced with pathogenic ADA2 variants were incubated with or without 2.5 µg/mL tunicamycin for 24h. ADA2 expression was measured by

western blot compared with GM-CSF-differentiated HMDM from a healthy control (HC) and two DADA2 patients (P). (B) ADA2 protein expression by western blot after glycan removal in ADA2$^{WT/WT}$ and ADA2$^{-/-}$ U-937 cells transduced with pathogenic ADA2 variants (*left*) and CD14+ monocytes or GM-CSF-differentiated HMDM from healthy controls (HC) and DADA2 patient P4 (*right*) by incubation with PNGase F or Endo H for 1 hour at 37°C under denaturing conditions. (C) α-mannosidases were inhibited by 72-96h incubation of ADA2$^{WT/WT}$ and ADA2$^{-/-}$ U-937 cells transduced with R169Q with 375 nM kifunensine and/or 10 μM swainsonine. ADA2 protein expression was determined by western blot. The histograms indicate molecular weight peaks as determined by Simple Western. The original graphs are provided in **Figures S10+S11**. (D) ADA2 protein expression by western blot GM-CSF- and M-CSF-differentiated HMDM from a healthy control (HC) and patient with α-mannosidosis (α-man) after incubation with 10 μM swainsonine for 96h. (E) ADA2 protein expression by western blot after glycan removal in ADA2$^{WT/WT}$ U-937 cells by incubation with PNGase F, Endo H or α1-2,3,6 Mannosidase for 1 hour at 37°C. Triangles indicate HMW-ADA2 (red), LMW-ADA2 (green) and glycan-free ADA2 (dark blue). Legend: EV, empty vector; NT, non-transfected, WT wild type.

differences between WT and mutant ADA2: Compared with mutant ADA2, Endo H-treated WT ADA2 visualized as a smear on western blot as opposed to the clean single band observed for mutant ADA2 in U-937 cells and HMDM (**Figure 7B**). This suggests that WT ADA2 underwent additional glycan processing as complex glycans are less sensitive to Endo H. Since the size of LMW-ADA2 makes the presence of additional carbohydrate residues unlikely, we concluded that in WT ADA2-expressing cells, the glycan trees of HMW-ADA2 mature into complex glycans, generating HMW(c)-ADA2, the HMW-form observed in HC HMDM. For all tested pathogenic variants, glycan removal by Endo H yielded a clean band very close in molecular weight to complete removal of N-glycans by PNGase F (**Figure 7B**). Consequently, mutant HMW-ADA2 is likely not subject to any glycan maturation beyond the ER, which is in agreement with the postulated ER retention of pathogenic ADA2 protein variants. This finding also implies that WT HMW(c)-ADA2 and mutant HMW-ADA2 – while very similar in molecular weight –differ in their glycan structures and do not represent the same ADA2 glycoform.

Collectively, our findings suggest that the N-glycan structures of ADA2 contain high-mannose oligosaccharides and that WT HMW(c)-ADA2 contains complex glycan branches while mutant HMW-ADA2 does not undergo advanced glycan maturation.

LMW-ADA2 is generated by glycan trimming through alpha-mannosidases

The addition of complex glycan structures is usually preceded by the removal of α-linked mannose residues in the late ER and Golgi by a set of α-mannosidases *(23)*. We therefore hypothesized that mutant ADA2 is inaccessible to glycan-trimming by endogenous α-mannosidases, accounting for the absence of complex glycan structures as well as the absence of LMW-ADA2. To test this hypothesis, we incubated WT and mutant ADA2-expressing U-937 cells with different inhibitors of glycan-processing enzymes. The corresponding western blots were performed in a capillary-based separation and detection system to allow for a more precise distinction of the different molecular weight peaks. After synthesis and N-glycan transfer in the ER, proteins are initially trimmed by the ER α-glucosidases I and II that are inhibited by castanospermine *(18)*. As shown in HMDM, castanospermine caused an increase in the molecular weight of HMW-ADA2 (**Figure S10**). By increasing the incubation time ≥ 48 hours we observed a shift also for LMW-ADA2, confirming the superior stability of LMW-ADA2 and the hypothesis that this glycoform is generated at a later stage of glycan processing. After passing the quality control mechanisms in the ER, proteins can be trimmed further by different α-mannosidases in the ER and Golgi. Kifunensine inhibits class I α-mannosidases that are typically found in the late ER and cis-Golgi and cleave α-1,2-linked mannose residues *(18)*. Incubation of U-937 cells with kifunensine led to an increase in the molecular weight of LMW-ADA2 (**Figure 7C** and **S11**). After 96 hours, LMW-ADA2 almost overlay HMW-ADA2 (**Figure 7C**). Concomitant incubation with swainsonine led to similar results. However, incubation with swainsonine alone also increased the molecular weight of LMW-ADA2, suggesting that multiple mannosidases are involved in the trimming of LMW-ADA2. Swainsonine inhibits both α-mannosidase II in the medial Golgi and the lysosomal α-mannosidase *(24)*. To better understand whether also the lysosomal enzyme is involved in the trimming of LMW-ADA2, we analyzed HMDM from a patient with α-mannosidosis, harbouring biallelic mutations in *MAN2B1* encoding the lysosomal α-mannosidase *(25)*. We found that the patient's cells phenocopied HC cells treated with the class II α-mannosidase inhibitor swainsonine and that

swainsonine treatment did not have an additional effect on the molecular weight of LMW-ADA2 expressed in the lysosomal α-mannosidase-deficient cells (**Figure 7D**). This finding suggests that LMW-ADA2 undergoes processing not only in the ER and Golgi but also in the lysosomes. The fact that HMW(c)-ADA2 expressed in the patient's HMDM appeared to undergo a slight shift towards a lower molecular weight upon addition of swainsonine might indicate that Golgi α-mannosidase II is involved in the maturation of the complex glycans of this glycoform (**Figure 7D**). Finally, as a proof of principle, we performed glycan removal by α1-2,3,6 mannosidase on WT ADA2. This experiment yielded a single band slightly lower but very close in molecular weight to LMW-ADA2 (**Figure 7E**). This is in line with the findings of the previous experiments since the inhibited glycan-processing enzymes typically do not cleave α-1,6-linked mannose residues, which accounts for the lower molecular weight of α1-2,3,6 mannosidase-treated ADA2 compared with LMW-ADA2 (**Figure 8**).

In summary, we demonstrated that LMW-ADA2 is generated from HMW-ADA2 by glycan-processing through multiple α-mannosidases in the ER, Golgi and lysosomal compartments.

Discussion

In this study, we showed that pathogenic protein variants of ADA2 expressed in HMDM from DADA2 patients do not undergo glycan processing beyond the ER and that DADA2 HMDM therefore lack lysosomal LMW-ADA2 and secreted HMW(c)-ADA2. We reported that the LMW-form represents an intracellular glycoform of ADA2 that is generated by α-mannosidase-mediated glycan cleavage after transport to the Golgi apparatus.

The importance of N-glycosylation in the trafficking and function of ADA2 has previously been established *(11, 12)*. Yet, the behavior of mutant ADA2 on the cellular level has to date only been examined in overexpression systems of cells that do not express the protein endogenously *(12, 13, 26)*. Importantly, expression of glycosyltransferases and glycosidases and therefore glycosylation

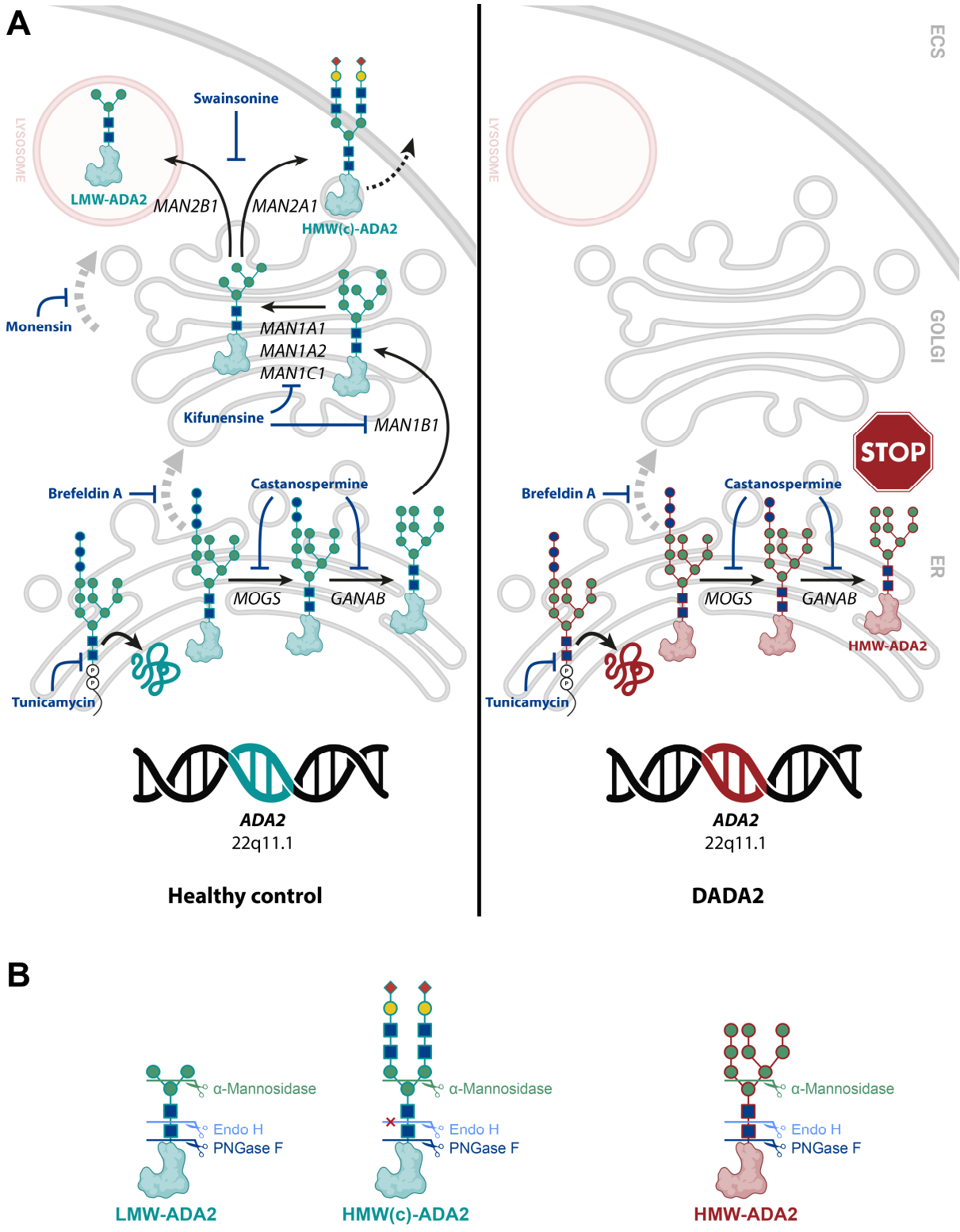

Figure 8: Processing of wild-type and mutant ADA2. (A) Schematic overview of the trafficking and glycan modifications of ADA2 expressed in healthy control (*left*) and DADA2 (*right*) human monocyte-derived macrophages based on the findings presented in this article. *MOGS* encodes ER α-glucosidase I, *GANAB* encodes ER α-glucosidase II, *MAN1B1* encodes ER α-1,2-mannosidase, *MAN1A1*, *MAN1A2* and *MAN1C1* encode Golgi α-1,2-mannosidases, *MAN2A1* encodes Golgi α-mannosidase II, and *MAN2B1* encodes lysosomal α-mannosidase. Mechanisms of action of the inhibitors used for the *in vitro* study of glycan processing are depicted in blue. (B) Cleavage sites of different endoglycosidases for the *in vitro* study of N-glycosylation. Endo H does not cleave

complex glycans (*middle*). Carbohydrate residues are depicted according to the Symbol Nomenclature for Glycans (SNFG) *(18)*. Legend: ECS, extracellular space; ER, endoplasmic reticulum.

patterns of individual proteins show striking variation even between different immune cell populations *(27)*. It is therefore essential to understand the behavior of ADA2 in the patients' primary cells. In our cohort of 10 DADA2 patients, we identified the intracellular predominance of unprocessed HMW-ADA2 in the absence of LMW-ADA2 as a feature that was shared by all missense variants, independently of the patients' clinical phenotype. Differential patterns of glycosylation of the same protein being associated with distinctive protein functions have previously been described: IL-24 is a signal peptide-containing glycoprotein that is secreted via the ER. A partially glycosylated cytosolic form of IL-24 has been shown to mediate protein kinase R activation independently of its extracellular function *(28)*. The predominance of the partially glycan-trimmed LMW-form of ADA2 in HC HMDM raises the question of whether, in a similar way, this form differs in function from secreted HMW(c)-ADA2. In fact, the function of ADA2 has repeatedly been subject to discussion for several reasons: (i.) Pathogenic ADA2 variants display a wide spectrum of residual adenosine deaminase function which does not clearly correlate with disease severity *(29)*. (ii.) ADA2 has evolved towards lower affinity to adenosine in higher species *(10)*. (iii.) ADA1 exhibits superior adenosine deaminase activity (Km of 20-50 μM vs. 2-3 mM for ADA2) and extracellular ADA1 bound to CD26 theoretically compensates for the absence of ADA2 at physiological levels of adenosine *(16)*. Yet, the majority of studies proposing possible pathomechanisms underlying the immunological phenotype of DADA2 rely on the role of ADA2 as an extracellular adenosine deaminase *(14, 15)*. In contrast, two groups introduced the possibility of an intracellular function of ADA2 as a lysosomal protein *(17, 30)*. Greiner-Tollersrud and colleagues characterized the glycan structures of ADA2 isolated from porcine brain and identified a high mannose-6-phosphate content, indicating targeting of ADA2 to the lysosome. Indeed, they showed an overlap between the glycosylation pattern of ADA2 with several known lysosomal

proteins *(17)*. We showed that the glycan structures of LMW- and HMW-ADA2 expressed in HMDM were sensitive to glycan removal by Endo H, suggesting the presence of high-mannose oligosaccharides *(31)*. This would be in line with a potential lysosomal localization of ADA2. Moreover, we showed that multiple – also lysosomal – α-mannosidases are involved in the processing of LMW-ADA2. Combined inhibition of class I and II α-mannosidases caused an increase in the molecular weight of LMW-ADA2 yielding a glycoform almost identical to HMW-ADA2. We proposed that the ADA2-glycoform observed in HC cells after inhibition of ER to Golgi trafficking might correspond to mutant HMW-ADA2. Yet, in most blots, DADA2 HMW-ADA2 looks identical in size to WT HMW(c)-ADA2. While the differential processing by Endo H clearly showed that the mutant protein does not undergo the same glycan maturation as HMW(c)-ADA2, the resolution of the western blots does not allow to definitively determine the precise molecular weight of the mutant protein. In the light of the complexity of glycan structures and glycan-processing enzymes, further analyses will be needed to define the exact composition of the LMW-ADA2 glycoform. Whether the predominant intracellular LMW-form of ADA2 that we detected in HMDM represents this lysosomal protein cannot be conclusively established from our data. Due to insufficient pull-down of LMW-ADA2 by immunoprecipitation, we could not elucidate its interactome and approach its potential function in this way. We did however detect LMW-ADA2 in the lysosomal compartment of U-937 cells after lysosomal enrichment. The subcellular fractionation experiments provide only an approximation of the intracellular localization of LMW-ADA2 since the enriched fractions are not sufficiently pure to exclude interfractional contamination. Combined with the previous studies *(17, 30)*, our data provide a strong hint that LMW-ADA2 represents the lysosomal glycoform of ADA2 and might be functionally distinct from secreted HMW(c)-ADA2.

In the HEK293T model system, transfected ADA2 was predominantly expressed as the HMW-form corresponding to secreted ADA2 in these cells, highlighting the limitations of this system to understand the behavior of endogenous ADA2. Discrepancies between the two systems are also

evident from the fact that ADA2 in whole cell lysates from transfected HEK293T cells was equally sensitive to glycan removal by PNGase F or Endo H *(12)*, while we observed some residual glycan structures upon Endo H treatment of ADA2 in lysates from U-937 cells and HMDM (**Figure 7B**). Another limitation of the relevance of macrophage LMW-ADA2 in the pathogenesis of DADA2 is that in primary CD14+ monocytes, the cells with the highest endogenous expression of ADA2, differentially glycosylated forms of ADA2 cannot be clearly distinguished (**Figure 1A+B**). Moreover, patient monocytes – both from patients with missense variants with normal *ADA2* mRNA expression and from patients with variants that exhibit nonsense-mediated mRNA decay – show complete absence of mutant ADA2 protein expression. This implies that mutations in the *ADA2* gene might manifest differently on a cellular level depending on the expressing cell.

This notion needs to be taken into account when examining the potential induction of ER stress by pathogenic variants of ADA2. Intracellular retention of ADA2 has only been reported after overexpression in HEK293T cells *(2, 13)*. While primary monocytic cells also show impaired secretion of mutant ADA2, intracellular protein levels are very low in HMDM and close to absent in CD14+ monocytes. In our cohort of DADA2 patients, we did not observe an increased ER stress response in CD14+ monocytes. This was in line with single-cell RNA-sequencing data reported by Watanabe et al. that showed downregulation of eIF2 signaling – a main pathway of the integrated stress response *(32, 33)*.

Although we could not confirm that the presence of misfolded mutant ADA2 contributes to the pathophysiology of the disease by induction of an unfolded protein response, our data highlight the need for a better understanding of the folding and trafficking mechanisms of WT and mutant ADA2. We verified that the presence of pathogenic ADA2 protein variants as well as inhibition of N-glycosylation provoked the formation of intracellular protein aggregates, thereby extending previous reports *(12, 26)*. In addition, we showed that aggregate formation also occurs after co-transfection in the presence of the wild-type protein. These findings offer a possible explanation for heterozygous carriers presenting with clinical symptoms and underscore the importance of

gaining in-depth understanding of the intracellular pathophysiology of DADA2. Next to Sanger sequencing of the *ADA2* gene, the measurement of serum ADA2 enzyme activity currently represents the diagnostic gold standard for DADA2. Assuming an intracellular function of the protein, it is possible that this strategy may overlook a proportion of patients. In this article, we introduced the absence of LMW-ADA2 as a new characteristic of pathogenic *ADA2* variants that was verified for all pathogenic variants included in this study. Despite the focus on pathogenic missense variants in our cohort, we propose the absence of LMW-ADA2 as cellular feature of DADA2 since complete loss of ADA2 protein expression due nonsense-mediated mRNA decay also leads to absence of this form. Our findings suggest a possible role of LMW-ADA2 as a biomarker in DADA2, which would need further validation in a larger set of pathogenic and benign *ADA2* variants.

Until now, monocytes as the main producers of endogenous ADA2 have received the most attention in deciphering the pathophysiology of the disease. Considering the role of glycosylation in protein folding and the potential impact of this modification on protein function, we cannot exclude that the main ADA2 function might vary even between different immune cells. This might also account for the diverse clinical phenotype of the disease and the varying involvement of different immune cell populations. The large number of pathogenic variants and their diversity with respect to biochemical characteristics are additional factors contributing to the difficulties in delineating a single all-encompassing pathomechanism that explains the complexity of the disease.

In conclusion, we demonstrate for the first time the differential N-glycosylation of pathogenic ADA2 in patient-derived macrophages. We establish LMW-ADA2 as a hypoglycosylated non-secreted form of ADA2 in healthy controls. This LMW-ADA2 is generated by α-mannosidases after transfer to the Golgi and is absent in DADA2. Further studies will be needed to confirm the functional relevance of these results in the pathogenesis of the disease.

Materials and methods

Study design

This exploratory study included patients treated at University Hospitals Leuven and their parents were included as heterozygous carriers. The diagnosis of DADA2 was made based on the clinical phenotype followed by a combination of serum ADA2 enzyme activity and sequencing of the *ADA2* gene according to the DADA2 management guidelines *(34)*. Healthy donors were recruited at University Hospitals Leuven and KU Leuven. This study was approved by the Ethics Committee for Research of Leuven University Hospitals (project numbers S63077, S63807). The patient with α-mannosidosis was recruited at Charité University Hospital in Berlin. The inclusion of the patient from Berlin was approved by the Ethics Committee of Charité University Medicine Berlin (project number EA2/1178/22). The patients provided written informed consent prior to participation. It was performed in accordance with the ethical standards as laid down in the 1964 Declaration of Helsinki and its later amendments. Our study examined male and female individuals, and similar findings are reported for both sexes.

The aim of this study was to determine the protein characteristics of ADA2 endogenously expressed in human immune cells carrying pathogenic *ADA2* variants. To compensate for the limited sample size in the study of patients with rare diseases, our results were validated in two separate *in vitro* models of ADA2 deficiency examining a total of 11 pathogenic *ADA2* variants. The results were confirmed using two different anti-ADA2 antibodies both validated with the help of ADA2 knockout samples and reproduced in two technically distinct blotting systems to exclude technical artefacts.

Immunoblotting

Adherent cells were detached with trypsin-EDTA (0.05%) (#25300062; Gibco) for 5 minutes at 37°C and the reaction was blocked by addition of complete medium. Cells were pelleted by

centrifugation at 400xg for 5 minutes at 4°C. Whole cell lysates were obtained by lysing $1x10^6$ cells in 25 µL RIPA buffer (150 mM NaCl, 1% Triton X-100, 0.5% sodium deoxycholate, 0.1% SDS, pH 8.0) or NP-40 lysis buffer (150 mM NaCl, 50 mM Tris-HCl, 1% NP-40, pH 7.4) containing protease inhibitor (#78429; Thermo Fisher Scientific) for 30 minutes on ice, followed by centrifugation at 13,500xg for 20 minutes at 4°C.

To collect supernatants, cells were cultured in serum-free medium for 24h. For immunoblotting, supernatants were concentrated by added 1200 µL ice-cold acetone to 300 µL supernatant and overnight storage at -20°C. Supernatant proteins were then precipitated by centrifugation at 15,000xg for 15 minutes at 4°C. The protein pellet was resuspended in 25 µL NP-40 buffer containing protease inhibitor. Bolt™ LDS sample buffer (#B0007; Thermo Fisher Scientific) mixed with Bolt™ Sample Reducing Agent (#B0009; Thermo Fisher Scientific) was added to the samples prior to gel electrophoresis. For analysis of intracellular dimer formation, the reducing agent was omitted. Samples were heated for 5 minutes at 70°C. Supernatants from HEK293T cells transfected with ADA2 were diluted 1:10 in 2X Bolt™ LDS sample buffer (#B0007; Thermo Fisher Scientific), serum was diluted 1:200. SeeBlue™ Plus2 Pre-stained Protein Standard (#LC5925; Thermo Fisher Scientific) was used as protein molecular weight marker.

Proteins were transferred onto PVDF transfer membranes. Protein expression was visualized by enzymatic chemiluminescence using Pierce™ ECL western blotting substrate (#32106; Thermo Fisher Scientific) or SuperSignal™ West Pico PLUS Chemiluminescent Substrate (#34580; Thermo Fisher Scientific) in a ChemiDoc XRS+ Imaging System (Bio-Rad).

The experiments examining the glycan-processing of LMW-ADA2 were performed in a Wes Automated Western Blot System (ProteinSimple / bio-techne) according to the manufacturer's instructions. Sample were loaded at a final protein concentration of 0.4 mg/mL.

Glycan removal

Glycan removal was performed on whole cell lysates generated with NP-40 lysis buffer or precipitated supernatant protein reconstituted in NP-40 lysis buffer. Glycan removal was performed on 20 μg, 10 μg or 25 μg total protein using PNGase F (#P0704; New England Biolabs), Endo H (#P0702; New England Biolabs), α1-2,3,6 Mannosidase (#P0768; New England Biolabs) or PNGase F (#A39245; Gibco) according to the manufacturer's instructions. Glycan removal with PNGase F (#P0704; New England Biolabs) was completed under denaturing conditions for 1h at 37°C or under non-denaturing conditions for 4h at 37°C as indicated.

Statistics

For the SomaScan assay, raw counts expressed in relative fluorescent units (RFU) were normalized across samples using a cyclic loess algorithm implemented by the package limma *(35)*. Two outlier samples identified with principal component analysis were removed before downstream analysis. Differentially expressed genes were identified using a linear model based on subject condition (HC, Carrier, DADA2), subject age, and number of freeze-thaw-cycles of the sample. Pseudoreplicates coming from subjects with multiple samples were handled using blocking. Statistics were moderated using the empirical Bayes method of the package limma *(35)*.

Statistical analysis of the mass spectrometry data was performed using Perseus software (v1.6.2.1) *(36)*. Log2 transformed LFQ intensity values were filtered for minimum of 3 valid values in at least one experimental group and missing values were imputed with random low intensity values taken from a normal distribution. Differences in protein abundance between groups were calculated using two-sample Student's t-test using an FDR-based significance cut-off of 5% (*HEK293T*) or 10% (*HMDM*) in order to define enriched proteins.

A complete description of all additional methods is provided in the Supplementary Materials.

References

1. Q. Zhou, D. Yang, A. K. Ombrello, A. V. Zavialov, C. Toro, A. V. Zavialov, D. L. Stone, J. J. Chae, S. D. Rosenzweig, K. Bishop, K. S. Barron, H. S. Kuehn, P. Hoffmann, A. Negro, W. L. Tsai, E. W. Cowen, W. Pei, J. D. Milner, C. Silvin, T. Heller, D. T. Chin, N. J. Patronas, J. S. Barber, C.-C. R. Lee, G. M. Wood, A. Ling, S. J. Kelly, D. E. Kleiner, J. C. Mullikin, N. J. Ganson, H. H. Kong, S. Hambleton, F. Candotti, M. M. Quezado, K. R. Calvo, H. Alao, B. K. Barham, A. Jones, J. F. Meschia, B. B. Worrall, S. E. Kasner, S. S. Rich, R. Goldbach-Mansky, M. Abinun, E. Chalom, A. C. Gotte, M. Punaro, V. Pascual, J. W. Verbsky, T. R. Torgerson, N. G. Singer, T. R. Gershon, S. Ozen, O. Karadag, T. A. Fleisher, E. F. Remmers, S. M. Burgess, S. L. Moir, M. Gadina, R. Sood, M. S. Hershfield, M. Boehm, D. L. Kastner, I. Aksentijevich, Early-onset stroke and vasculopathy associated with mutations in ADA2. *N. Engl. J. Med.* **370**, 911–920 (2014).
2. P. Navon Elkan, S. B. Pierce, R. Segel, T. Walsh, J. Barash, S. Padeh, A. Zlotogorski, Y. Berkun, J. J. Press, M. Mukamel, I. Voth, P. J. Hashkes, L. Harel, V. Hoffer, E. Ling, F. Yalcinkaya, O. Kasapcopur, M. K. Lee, R. E. Klevit, P. Renbaum, A. Weinberg-Shukron, E. F. Sener, B. Schormair, S. Zeligson, D. Marek-Yagel, T. M. Strom, M. Shohat, A. Singer, A. Rubinow, E. Pras, J. Winkelmann, M. Tekin, Y. Anikster, M.-C. King, E. Levy-Lahad, Mutant adenosine deaminase 2 in a polyarteritis nodosa vasculopathy. *N. Engl. J. Med.* **370**, 921–931 (2014).
3. I. Meyts, I. Aksentijevich, Deficiency of Adenosine Deaminase 2 (DADA2): Updates on the Phenotype, Genetics, Pathogenesis, and Treatment. *J. Clin. Immunol.* **38**, 569–578 (2018).
4. K. J. Karczewski, L. C. Francioli, G. Tiao, B. B. Cummings, J. Alföldi, Q. Wang, R. L. Collins, K. M. Laricchia, A. Ganna, D. P. Birnbaum, L. D. Gauthier, H. Brand, M. Solomonson, N. A. Watts, D. Rhodes, M. Singer-Berk, E. M. England, E. G. Seaby, J. A. Kosmicki, R. K. Walters, K. Tashman, Y. Farjoun, E. Banks, T. Poterba, A. Wang, C. Seed, N. Whiffin, J. X. Chong, K. E. Samocha, E. Pierce-Hoffman, Z. Zappala, A. H. O'Donnell-Luria, E. V. Minikel, B. Weisburd, M. Lek, J. S. Ware, C. Vittal, I. M. Armean, L. Bergelson, K. Cibulskis, K. M. Connolly, M. Covarrubias, S. Donnelly, S. Ferriera, S. Gabriel, J. Gentry, N. Gupta, T. Jeandet, D. Kaplan, C. Llanwarne, R. Munshi, S. Novod, N. Petrillo, D. Roazen, V. Ruano-Rubio, A. Saltzman, M. Schleicher, J. Soto, K. Tibbetts, C. Tolonen, G. Wade, M. E. Talkowski, B. M. Neale, M. J. Daly, D. G. MacArthur, The mutational constraint spectrum quantified from variation in 141,456 humans. *Nature* **581**, 434–443 (2020).
5. Infevers: an online database for autoinflammatory mutations. Copyright. Available at https://infevers.umai-montpellier.fr/ Accessed 17/08/2024. (available at https://infevers.umai-montpellier.fr/web/instructions_for_use.php).
6. P. Y. Lee, E. S. Kellner, Y. Huang, E. Furutani, Z. Huang, W. Bainter, M. F. Alosaimi, K. Stafstrom, C. D. Platt, T. Stauber, S. Raz, I. Tirosh, A. Weiss, M. B. Jordan, C. Krupski, D. Eleftheriou, P. Brogan, A. Sobh, Z. Baz, G. Lefranc, C. Irani, S. S. Kilic, R. El-Owaidy, M. R. Lokeshwar, P. Pimpale, R. Khubchandani, E. P. Chambers, J. Chou, R. S. Geha, P. A. Nigrovic, Q. Zhou, Genotype and functional correlates of disease phenotype in deficiency of adenosine deaminase 2 (DADA2). *J. Allergy Clin. Immunol.* **145**, 1664-1672.e10 (2020).
7. M. Dzhus, L. Ehlers, M. Wouters, K. Jansen, R. Schrijvers, L. De Somer, S. Vanderschueren, M. Baggio, L. Moens, B. Verhaaren, R. Lories, G. Bucciol, I. Meyts, A Narrative Review of the

Neurological Manifestations of Human Adenosine Deaminase 2 Deficiency. *J. Clin. Immunol.* (2023), doi:10.1007/s10875-023-01555-y.

8. N. T. Deuitch, D. Yang, P. Y. Lee, X. Yu, N. S. Moura, O. Schnappauf, A. K. Ombrello, D. Stone, H. S. Kuehn, S. D. Rosenzweig, P. Hoffmann, C. Cudrici, D. M. Levy, E. Kessler, J. B. Soep, A. D. Hay, A. Dalrymple, Y. Zhang, L. Sun, Q. Zhang, X. Tang, Y. Wu, K. Rao, H. Li, H. Luo, Y. Zhang, J. M. Burnham, M. Boehm, K. Barron, D. L. Kastner, I. Aksentijevich, Q. Zhou, TNF inhibition in vasculitis management in adenosine deaminase 2 deficiency (DADA2). *J. Allergy Clin. Immunol.* **149**, 1812-1816.e6 (2022).
9. H. Hashem, A. R. Kumar, I. Müller, F. Babor, R. Bredius, J. Dalal, A. P. Hsu, S. M. Holland, D. D. Hickstein, S. Jolles, R. Krance, G. Sasa, M. Taskinen, M. Koskenvuo, J. Saarela, J. van Montfrans, K. Wilson, B. Bosch, L. Moens, M. Hershfield, I. Meyts, Hematopoietic stem cell transplantation rescues the hematological, immunological, and vascular phenotype in DADA2. *Blood* **130**, 2682–2688 (2017).
10. A. V. Zavialov, X. Yu, D. Spillmann, G. Lauvau, A. V. Zavialov, Structural basis for the growth factor activity of human adenosine deaminase ADA2. *J. Biol. Chem.* **285**, 12367–12377 (2010).
11. P. Y. Lee, Y. Huang, Q. Zhou, O. Schnappauf, M. S. Hershfield, Y. Li, N. J. Ganson, N. Sampaio Moura, O. M. Delmonte, S. S. Stone, M. J. Rivkin, S.-Y. Pai, T. Lyons, R. P. Sundel, V. W. Hsu, L. D. Notarangelo, I. Aksentijevich, P. A. Nigrovic, Disrupted N-linked glycosylation as a disease mechanism in deficiency of ADA2. *J. Allergy Clin. Immunol.* **142**, 1363-1365.e8 (2018).
12. M. Ito, Y. Maejima, K. Nishimura, Y. Nakae, A. Ono, S. Iwaki-Egawa, A role for N-glycosylation in active adenosine deaminase 2 production. *Biochim. Biophys. Acta BBA - Gen. Subj.* **1866**, 130237 (2022).
13. L. Chen, A. Mamutova, A. Kozlova, E. Latysheva, F. Evgeny, T. Latysheva, K. Savostyanov, A. Pushkov, I. Zhanin, E. Raykina, M. Kurnikova, I. Mersiyanova, C. D. Platt, H. Jee, K. Brodeur, Y. Du, M. Liu, A. Weiss, G. S. Schulert, J. Rodriguez-Smith, M. S. Hershfield, I. Aksentijevich, Q. Zhou, P. A. Nigrovic, A. Shcherbina, E. Alexeeva, P. Y. Lee, Comparison of disease phenotypes and mechanistic insight on causal variants in patients with DADA2. *J. Allergy Clin. Immunol.* (2023), doi:10.1016/j.jaci.2023.04.014.
14. C. Carmona-Rivera, S. S. Khaznadar, K. W. Shwin, J. A. Irizarry-Caro, L. J. O'Neil, Y. Liu, K. A. Jacobson, A. K. Ombrello, D. L. Stone, W. L. Tsai, D. L. Kastner, I. Aksentijevich, M. J. Kaplan, P. C. Grayson, Deficiency of adenosine deaminase 2 triggers adenosine-mediated NETosis and TNF production in patients with DADA2. *Blood* **134**, 395–406 (2019).
15. R. Dhanwani, M. Takahashi, I. T. Mathews, C. Lenzi, A. Romanov, J. D. Watrous, B. Pieters, C. C. Hedrick, C. A. Benedict, J. Linden, R. Nilsson, M. Jain, S. Sharma, Cellular sensing of extracellular purine nucleosides triggers an innate IFN-β response. *Sci. Adv.* **6**, eaba3688 (2020).
16. T. K. Tarrant, S. J. Kelly, M. S. Hershfield, Elucidating the pathogenesis of adenosine deaminase 2 deficiency: current status and unmet needs. *Expert Opin. Orphan Drugs* **9**, 257–264 (2021).
17. O. K. Greiner-Tollersrud, V. Boehler, E. Bartok, M. Krausz, A. Polyzou, J. Schepp, M. Seidl, J. O. Olsen, C. R. Smulski, S. Raieli, K. Hübscher, E. Trompouki, R. Link, H. Ebersbach, H. Srinivas, M. Marchant, D. Staab, D. Guerini, S. Baasch, P. Henneke, G. Kochs, G. Hartmann, R. Geiger, B. Grimbacher, M. Warncke, M. Proietti, *ADA2 is a lysosomal DNase regulating the type-I interferon response* (2020; https://www.biorxiv.org/content/10.1101/2020.06.21.162990v2), p. 2020.06.21.162990.

18. A. Varki, R. D. Cummings, J. D. Esko, P. Stanley, G. W. Hart, M. Aebi, D. Mohnen, T. Kinoshita, N. H. Packer, J. H. Prestegard, R. L. Schnaar, P. H. Seeberger, Eds., *Essentials of Glycobiology* (Cold Spring Harbor Laboratory Press, Cold Spring Harbor (NY), ed. 4th, 2022; http://www.ncbi.nlm.nih.gov/books/NBK579918/).
19. N. Louros, J. Schymkowitz, F. Rousseau, Mechanisms and pathology of protein misfolding and aggregation. *Nat. Rev. Mol. Cell Biol.* **24**, 912–933 (2023).
20. P. Kirchner, M. Bourdenx, J. Madrigal-Matute, S. Tiano, A. Diaz, B. A. Bartholdy, B. Will, A. M. Cuervo, Proteome-wide analysis of chaperone-mediated autophagy targeting motifs. *PLOS Biol.* **17**, e3000301 (2019).
21. T. Fujiwara, K. Oda, S. Yokota, A. Takatsuki, Y. Ikehara, Brefeldin A causes disassembly of the Golgi complex and accumulation of secretory proteins in the endoplasmic reticulum. *J. Biol. Chem.* **263**, 18545–18552 (1988).
22. H. H. Mollenhauer, D. James Morré, L. D. Rowe, Alteration of intracellular traffic by monensin; mechanism, specificity and relationship to toxicity. *Biochim. Biophys. Acta BBA - Rev. Biomembr.* **1031**, 225–246 (1990).
23. K. Legler, R. Rosprim, T. Karius, K. Eylmann, M. Rossberg, R. M. Wirtz, V. Müller, I. Witzel, B. Schmalfeldt, K. Milde-Langosch, L. Oliveira-Ferrer, Reduced mannosidase MAN1A1 expression leads to aberrant N-glycosylation and impaired survival in breast cancer. *Br. J. Cancer* **118**, 847–856 (2018).
24. D. R. Rose, Structure, mechanism and inhibition of Golgi α-mannosidase II. *Curr. Opin. Struct. Biol.* **22**, 558–562 (2012).
25. D. Malm, Ø. Nilssen, Alpha-mannosidosis. *Orphanet J. Rare Dis.* **3**, 21 (2008).
26. S. M. Bowers, M. Sundqvist, P. Dancey, D. A. Cabral, K. L. Brown, Pathogenic variant c.1052T>A (p.Leu351Gln) in adenosine deaminase 2 impairs secretion and elevates type I IFN responsive gene expression. *Front. Immunol.* **13** (2022) (available at https://www.frontiersin.org/articles/10.3389/fimmu.2022.995191).
27. M. A. Daniels, K. A. Hogquist, S. C. Jameson, Sweet "n" sour: the impact of differential glycosylation on T cell responses. *Nat. Immunol.* **3**, 903–910 (2002).
28. S. Davidson, C.-H. Yu, A. Steiner, F. Ebstein, P. J. Baker, V. Jarur-Chamy, K. Hrovat Schaale, P. Laohamonthonkul, K. Kong, D. J. Calleja, C. R. Harapas, K. R. Balka, J. Mitchell, J. T. Jackson, N. D. Geoghegan, F. Moghaddas, K. L. Rogers, K. D. Mayer-Barber, A. A. De Jesus, D. De Nardo, B. T. Kile, A. J. Sadler, M. C. Poli, E. Krüger, R. Goldbach Mansky, S. L. Masters, Protein kinase R is an innate immune sensor of proteotoxic stress via accumulation of cytoplasmic IL-24. *Sci. Immunol.* **7**, eabi6763 (2022).
29. H. Jee, Z. Huang, S. Baxter, Y. Huang, M. L. Taylor, L. A. Henderson, S. Rosenzweig, A. Sharma, E. P. Chambers, M. S. Hershfield, Q. Zhou, F. Dedeoglu, I. Aksentijevich, P. A. Nigrovic, A. O'Donnell-Luria, P. Y. Lee, Comprehensive analysis of ADA2 genetic variants and estimation of carrier frequency driven by a function-based approach. *J. Allergy Clin. Immunol.* (2021), doi:10.1016/j.jaci.2021.04.034.
30. L. Dong, W. Luo, S. Maksym, S. C. Robson, A. V. Zavialov, Adenosine deaminase 2 regulates the activation of the toll-like receptor 9 in response to nucleic acids. *Front. Med.* (2024), doi:10.1007/s11684-024-1067-5.
31. M.-S. Kim, D. Leahy, in *Methods in Enzymology*, Laboratory Methods in Enzymology: Cell, Lipid and Carbohydrate. J. Lorsch, Ed. (Academic Press, 2013), vol. 533, pp. 259–263.

32. N. Watanabe, S. Gao, Z. Wu, S. Batchu, S. Kajigaya, C. Diamond, L. Alemu, D. Q. Raffo, P. Hoffmann, D. Stone, A. K. Ombrello, N. S. Young, Analysis of deficiency of adenosine deaminase 2 pathogenesis based on single-cell RNA sequencing of monocytes. *J. Leukoc. Biol.* **110**, 409–424 (2021).
33. K. Pakos-Zebrucka, I. Koryga, K. Mnich, M. Ljujic, A. Samali, A. M. Gorman, The integrated stress response. *EMBO Rep.* **17**, 1374–1395 (2016).
34. P. Y. Lee, B. A. Davidson, R. S. Abraham, B. Alter, J. I. Arostegui, K. Bell, A. Belot, J. R. E. Bergerson, T. J. Bernard, P. A. Brogan, Y. Berkun, N. T. Deuitch, D. Dimitrova, S. A. Georgin-Lavialle, M. Gattorno, B. Grimbacher, H. Hashem, M. S. Hershfield, R. N. Ichord, K. Izawa, J. A. Kanakry, R. P. Khubchandani, F. C. C. Klouwer, E. A. Luton, A. W. Man, I. Meyts, J. M. Van Montfrans, S. Ozen, J. Saarela, G. C. Santo, A. Sharma, A. Soldatos, R. Sparks, T. R. Torgerson, I. L. Uriarte, T. A. B. Youngstein, Q. Zhou, I. Aksentijevich, D. L. Kastner, E. P. Chambers, A. K. Ombrello, DADA2 Foundation, Evaluation and Management of Deficiency of Adenosine Deaminase 2: An International Consensus Statement. *JAMA Netw. Open* **6**, e2315894 (2023).
35. M. E. Ritchie, B. Phipson, D. Wu, Y. Hu, C. W. Law, W. Shi, G. K. Smyth, limma powers differential expression analyses for RNA-sequencing and microarray studies. *Nucleic Acids Res.* **43**, e47 (2015).
36. S. Tyanova, T. Temu, P. Sinitcyn, A. Carlson, M. Y. Hein, T. Geiger, M. Mann, J. Cox, The Perseus computational platform for comprehensive analysis of (prote)omics data. *Nat. Methods* **13**, 731–740 (2016).
37. J. G. Doench, N. Fusi, M. Sullender, M. Hegde, E. W. Vaimberg, K. F. Donovan, I. Smith, Z. Tothova, C. Wilen, R. Orchard, H. W. Virgin, J. Listgarten, D. E. Root, Optimized sgRNA design to maximize activity and minimize off-target effects of CRISPR-Cas9. *Nat. Biotechnol.* **34**, 184–191 (2016).
38. J. Rappsilber, Y. Ishihama, M. Mann, Stop and go extraction tips for matrix-assisted laser desorption/ionization, nanoelectrospray, and LC/MS sample pretreatment in proteomics. *Anal. Chem.* **75**, 663–670 (2003).
39. S. Tyanova, T. Temu, J. Cox, The MaxQuant computational platform for mass spectrometry-based shotgun proteomics. *Nat Protoc* **11**, 2301–2319 (2016).
40. J. Illingworth, Methods of enzymatic analysis: Third edition: Editor-in-Chief: Hans Ulrich Bergmeyer. Verlag Chemie, 1983 (vols I–III), 1984 (vols IV & V) DM258 each volume or DM2240 vols I–X inclusive. *Biochem. Educ.* **13**, 38–38 (1985).
41. K. J. Livak, T. D. Schmittgen, Analysis of relative gene expression data using real-time quantitative PCR and the 2(-Delta Delta C(T)) Method. *Methods San Diego Calif* **25**, 402–408 (2001).
42. H. H. Freeze, Towards a therapy for phosphomannomutase 2 deficiency, the defect in CDG-Ia patients. *Biochim. Biophys. Acta BBA - Mol. Basis Dis.* **1792**, 835–840 (2009).
43. T. Bachetti, S. Chiesa, P. Castagnola, D. Bani, E. D. Zanni, A. Omenetti, A. D'Osualdo, A. Fraldi, A. Ballabio, R. Ravazzolo, A. Martini, M. Gattorno, I. Ceccherini, Autophagy contributes to inflammation in patients with TNFR-associated periodic syndrome (TRAPS). *Ann. Rheum. Dis.* **72**, 1044–1052 (2013).

Acknowledgments

We thank Prof. Jaak Jaeken, Prof. Daisy Rymen and Dr. Eva Morava-Kozicz for kindly sharing their expertise and insight on protein glycosylation. We thank Lotte Bral for her assistance in the production of the knock-out cell lines and Julia Neugebauer for her help with the sample collection. Above all, we would like to express our gratitude to our patients and their parents for their willingness to participate in our study and to their treating physicians and nurses for their efforts in the collection of research samples. The graphical abstract was created with BioRender.com.

Funding

This project has received funding from the following sources:

European Research Council (ERC) under the European Union's Horizon 2020 research and innovation program GA No. 948959 (MORE2ADA2) (LE, MW, BP, MD, IM)

KU Leuven C1 Grant C16/18/007 (IM)

Research Foundation-Flanders (FWO) grant G0B5120N (IM)

Jeffrey Modell Foundation (IM)

ERN-RITA (IM)

Research Foundation – Flanders (FWO) grant 11E0123N (LE)

Charité – Universitätsmedizin Berlin and the Berlin Institute of Health BIH Charité Junior Clinician Scientist Fellowship (LE)

Research Foundation – Flanders (FWO) grant 11F4421N (SD)

Research Foundation – Flanders (FWO) grant 1805523N (RS)

Research Foundation – Flanders (FWO) grant G0A3320N (PA)

KU Leuven C14/21/095 InterAction consortium (PA)

EOS MetaNiche consortium N° 40007532 (PA)

iBOF/21/053 ATLANTIS network (PA)

EOS DECODE consortium N° 30837538 (PA)

Author contributions

LE, LM and IM were responsible for the study conception and design. Material preparation and data collection was performed by LE, AH, MW, BP, SD, MD, MK and LM. LE, AH, MB, MK and LM performed the data analysis. MJ and DD assisted in the generation of ADA2 knock-out cell lines. The proteomics analyses were performed in collaboration with MK, PM, MFM and TM. FE was involved in the design of the trafficking experiments. PA supported the design of the ER stress experiments. LE, SD, GB, LDS, RS, SV, DC and IM collected clinical data and biological materials from patients. The manuscript was written by LE. All authors reviewed the manuscript and approved its submission. IM is responsible for the supervision of the study.

Competing interests

IM receives research funding from CSL-Behring outside this project. Other grant support was received from Octapharma, as well as Advisory Board honoraries from Takeda and Boehringer-Ingelheim - paid to the institution and outside the submitted work.

Data and materials availability

The mass spectrometry data have been deposited to the ProteomeXchange Consortium via the PRIDE partner repository with the dataset identifier PXD046128. Further information are available upon request.

Tables

ID	Age [years]	Sex	Genotype	Predominant phenotype
P1	12	M	c.973-2A>G/c.del1240-1442; splice site (intron 6)/del exon 9	Vasculitis, hepatosplenomegaly, hypogammaglobulinemia
P2	14	F	c.973-2A>G/c.del1240-1442; splice site (intron 6)/del exon 9	Vasculitis, warts, hypogammaglobulinemia, arthralgia
P3	26	M	c.140G>T/c.del1240-1442; p.G47V/del exon 9	Bone marrow failure, hypogammaglobulinemia, hepatosplenomegaly
P4	26	M	c.140G>T/c.140G>T; p.G47V/p.G47V	Hypogammaglobulinemia, hepatosplenomegaly
P5	6	F	c.140G>T/c.506G>A; p.G47V/p.R169Q	Hypogammaglobulinemia, hepatosplenomegaly, stroke
P6	9	F	c.140G>T/c.506G>A; p.G47V/p.R169Q	Bone marrow failure, hypogam-maglobulinemia, hepatosplenomegaly
P7	32	F	c.973-2A>G/c.506G>A; splice site (intron 6)/p.R169Q	Stroke, hypertension
P8	16	M	c.139G>A/c.139G>A; p.G47R/p.G47R	Stroke, vasculitis
P9	10	F	c.973-2A>G/c.973-2A>G; splice site (intron 6)/splice site (intron 6)	Vasculitis, hypogammaglobulinemia
P10	50	F	c.973-2A>G/c.506G>A; splice site (intron 6)/p.R169Q	Vasculitis, leukopenia
CR1	39	F	WT/c. del1240-1442; WT/del exon 9	
CR2	38	F	WT/c.140G>T; WT/p.G47V	
CR3	42	M	WT/c.506G>A; WT/p.R169Q	

Table 1. Cohort characteristics. Genotype and clinical phenotype of the included DADA2 patients (P) and heterozygous carriers (CR).